

ADA 035409

OFFICE OF NAVAL RESEARCH
Contract N00014-75-C-0794
Mod P00001

12
NW

TECHNICAL REPORT
LITHIUM GRAPHITE SECONDARY BATTERY

by

Douglas N. Bennion, Principal Investigator
and Sanjay L. Deshpande

Energy and Kinetics Department
School of Engineering and Applied Science
University of California
Los Angeles, California

December 1976

Distribution of this document is unlimited.

af
DDC
RECEIVED
FEB 7 1977
B

REPORT DOCUMENTATION PAGE

READ INSTRUCTIONS
BEFORE COMPLETING FORM

1. AUTHOR NUMBER

2. GOVT ACCESSION NO.

3. RECIPIENT'S CATALOG NUMBER

4. TITLE (and Subtitle)

Lithium-Graphite Secondary Battery

5. TYPE OF REPORT & PERIOD COVERED

Technical Report

6. PERFORMING ORGANIZATION REPORT NUMBER

UCLA-ENG-76127

7. CONTRACT OR GRANT NUMBER (S)

N00014-75-C-0794

Mod. P00001

8. AUTHOR (Last Name)

Douglas N. Bennion and Sanjay L. Deshpande

9. PERFORMING ORGANIZATION NAME AND ADDRESS

**School of Engineering and Applied Science,
University of California
Los Angeles, California**

10. CONTROLLING OFFICE NAME AND ADDRESS

**Office of Naval Research
Chemistry Program
Arlington, Virginia 22217**

11. MONITORING AGENCY NAME & ADDRESS (if different from Controlling Office)

1287

12. PROGRAM ELEMENT, PROJECT, TASK AREA & WORK UNIT NUMBERS

13. REPORT DATE

December 1976

14. NUMBER OF PAGES

15. SECURITY CLASS. (of this report)

Unlimited

16. DECLASSIFICATION/DOWNGRADING SCHEDULE

17. DISTRIBUTION STATEMENT (of this Report)

**Reproduction in whole or in part is permitted for any purpose of
the U.S. Government.**

18. DISTRIBUTION STATEMENT (of the abstract entered in Block 20, if different from Report)

19. SUPPLEMENTARY NOTES

20. KEY WORDS (Continue on reverse side if necessary and identify by block number)

**batteries, nonaqueous solvents, lithium perchlorate, dimethyl sulfite,
graphite, intercalation compound of graphite, radical cation of dimethyl
sulfite.**

21. ABSTRACT (Continue on reverse side if necessary and identify by block number)

**Reactions occurring at the positive and negative electrodes and in the
solution phase of cells of the type Li/LiClO₄, DMSU/Graphite have been
studied. Experiments were performed in an H-cell wherein the two electrodes
of the cell were isolated in compartments separated by a porous glass frit.
Discharge capability of 36 hours at a current density of 2 mA/cm² have been
demonstrated. Discharge potential was about 3.00 V measured versus a lithium
wire reference electrode. The effect of operating current on cell perform-
ance has been studied. The role of each component of the battery in the**

404121

20. Continued

charging and discharging reactions has been investigated.

Unlimited

PREFACE

This final report was prepared by Sanjay Deshpande, and Douglas N. Bennion, Principal Investigator. The work was done under contract number N0014-75-C-0794 Mod P00001 to the Regents of the University of California for the Office of Naval Research, Chemistry Program, Arlington, Virginia 22217.

ABSTRACT

Reactions occurring at the positive and negative electrodes and in the solution phase of cells of the type Li/LiClO_4 , DMSU/Graphite have been studied. Experiments were performed in an H-cell wherein the two electrodes of the cell were isolated in compartments separated by a porous glass frit. Discharge capability of 36 hours at a current density of 2 mA/cm^2 have been demonstrated. Discharge potential was about 3.00 V measured versus a lithium wire reference electrode. The effect of operating current on cell performance has been studied. The role of each component of the battery in the charging and discharging reactions has been investigated.

ACCESSION FOR	
DTIC	Wallo Section <input checked="" type="checkbox"/>
DDC	Defi Section <input type="checkbox"/>
UNANNOUNCED	<input type="checkbox"/>
JUSTIFICATION	
BY	
DISTRIBUTION/AVAILABILITY CODES	
Dist. AVAIL. and/or SPECIAL	
A	

TABLE OF CONTENTS

LIST OF CELLS	viii
LIST OF TABLES	ix
LIST OF FIGURES	x
CHAPTER 1. INTRODUCTION	1
Lithium nonaqueous battery systems	1
Lithium-Graphite battery	4
CHAPTER 2. EXPERIMENTAL	7
Materials	7
Apparatus	8
Preparation of positive electrode	12
Assembling the cell	13
Charging and discharging	14
CHAPTER 3. RESULTS	15
Measurements and observations	15
Preliminary experiments	16
Performance of the Li/ LiClO ₄ , DMSU/Graphite battery system	23
Demonstration of reversible electrical storage capacity	23
Effect of operating current	33
Specificity of the observed performance of the Lithium-Graphite battery system to its components	39
Electrolyte and solvent	39
Carbon or graphite in the pyrolyzed graphite positive electrode	55
Analysis of the solutions and the positive electrode	61

TABLE OF CONTENTS

(Continued)

Infra-red spectral analysis	61
X-Ray powder-diffraction analysis	62
Gas chromatographic analysis	65
CHAPTER 4. DISCUSSION	68
CHAPTER 5. CONCLUSIONS	76
REFERENCES	78

LIST OF CELLS

The following cells were used in preliminary experiments.

1. Li/LiClO_4 , DMSU (1.0M)/Graphite + Graphite glue on carbon cloth.
- 1a. Li/LiClO_4 , DMSU (1.0M)/Graphite + LiF + Graphite glue on carbon cloth.
2. Li/LiClO_4 , DMSU (1.0M)/Graphite + Teflon moulding powder on carbon cloth.
- 2a. Li/LiClO_4 , DMSU (1.0M)/Graphite + Teflon moulding powder on perforated Titanium foil.

The following cells were used in the main study.

3. Li/LiClO_4 , DMSU (1.0M)/Graphite + Graphite glue on carbon cloth.
Used in demonstration of reversible electrical storage capacity.
4. Cell same as 3, except that positive electrode was recycled.
Used in the trial experiment that studied the effect of operating current.
5. Cell same as 3. Used in the experiment that studied the effect of operating current.
6. Li/LiClO_4 , PC (0.9M)/Graphite + Graphite glue on carbon cloth.
7. Li/LiBF_4 , DMSU (1.0M)/Graphite + Graphite glue on carbon cloth.
8. Li/LiBF_4 , PC (1.5M)/Graphite + Graphite glue on carbon cloth.
9. Li/LiClO_4 , DMSU (2.1M)/Pt.
10. Li/LiClO_4 , DMSU (15M)/Graphite glue on carbon cloth.
11. Li/LiClO_4 , DMSU (2.1M)/Carbon cloth.

LIST OF TABLES

1. Room temperature nonaqueous battery systems using lithium negative electrodes.	
A. Primary systems	2
B. Secondary systems	3
2. Comparison of operating characteristics of Lithium-Graphite cell systems containing different electrolytic solutions.	53
3. Comparison of operating characteristics of Lithium-Graphite cell systems containing different positive electrodes.	60
4. Relative intensities of unidentified peaks in the x-ray powder diffraction patterns for samples of positive electrodes from different cells	63
5. Relative intensities of unidentified peaks in the x-ray powder diffraction patterns for samples of deposits on the negative electrode. Effect of purity of LiClO_4 used in the cell solution, LiClO_4 -DMSU	64
6. Chromatographic analysis of cell solutions and solvent. Column particulars and operating conditions	67
7. Chromatographic analysis of cell solutions and solvent. Variations in area under the peak with retention time of 60 seconds	67

LIST OF FIGURES

1. H-cell used in all experiments	10
2. Electrical circuit for charging and discharging	11
3. Typical galvanostatic charge discharge curves for the cell Li/LiClO_4 , DMSU (1.0 M)/Graphite + Graphite glue on carbon cloth	18
4. Typical galvanostatic charge discharge curves for the cell Li/LiClO_4 , DMSU (1.0 M)/Graphite + Teflon powder on carbon cloth	19
5. Galvanostatic charge discharge curves for the cell Li/LiClO_4 , DMSU (1.0 M)/Graphite + Teflon powder on Titanium	21
6. Typical galvanostatic charge discharge curves for the cell Li/LiClO_4 , DMSU (1.0 M)/Graphite + LiF + Graphite glue on carbon cloth	22
7. Galvanostatic charge discharge curves for the cell Li/LiClO_4 , DMSU (1.0 M)/Graphite + Graphite glue on carbon cloth.	
Cycle no. 1, $I=3.2 \text{ mA}$, $Q_{in}=1.30 \text{ mEq}$	24
8. Same as 7. Cycle no. 2, $I=6.3 \text{ mA}$, $Q_{in}=3.60 \text{ mEq}$	25
9. Same as 7. Cycle no. 3, $I=6.3 \text{ mA}$, $Q_{in}=6.23 \text{ mEq}$	26
10. Same as 7. Cycle no. 4, $I=6.3 \text{ mA}$, $Q_{in}=8.92 \text{ mEq}$	27
11. Effect of operating current density on coulombic efficiency (based on a cut off potential of $V_f = 2.00 \text{ V}$)	35
12. Effect of operating current density on the potential of the positive electrode versus the lithium wire reference electrode, V_2 , during the charging and discharging runs	36

LIST OF FIGURES

(Continued)

13.	Galvanostatic charge discharge curves for the cell Li/LiClO ₄ , PC (0.9 M)/Graphite+ Graphite glue on carbon cloth	
	Cycle no. 1, I=3.2 mA, Q _{in} =0.54 mEq	40
14.	Same as 13. Cycle no. 2, I=6.3 mA, Q _{in} =0.80 mEq	41
15.	Same as 13. Cycle no. 3, I=6.3 mA, Q _{in} =1.52 mEq	42
16.	Same as 13. Cycle no. 4, I=6.3 mA, Q _{in} =2.53 mEq	43
17.	Same as 13. Cycle no. 5, I=6.3 mA, Q _{in} =5.00 mEq	44
18.	Galvanostatic charge discharge curves for the cell Li/LiBF ₄ , DMSU (1.0 M)/Graphite+ Graphite glue on carbon cloth.	
	Cycle no. 1, I=3.2 mA, Q _{in} =1.09 mEq	45
19.	Same as 18. Cycle no. 2, I=6.3 mA, Q _{in} =2.44 mEq	46
21.	Same as 18. Cycle no. 3, I=6.3 mA, Q _{in} =4.16 mEq	47
22.	Same as 18. Cycle no. 4, I=6.3 mA, Q _{in} =1.85 mEq	48
23.	Galvanostatic discharge curves for the cell Li/LiBF ₄ , PC(1.5 M)/Graphite + Graphite glue on carbon cloth. Cycles 1 and 2	51
24.	Same as 23. Cycle no. 3, I=6.3 mA, Q _{in} =2.17 mEq	52
25.	Typical galvanostatic charge discharge curves for the cell Li/LiClO ₄ , DMSU (1.5 M)/Graphite glue on carbon cloth	57
26.	Galvanostatic discharge curves for the cell Li/LiClO ₄ , DMSU (2.1 M)/Carbon cloth, Cycles 1,2,3 and 4.	58

Chapter 1

INTRODUCTION

Lithium Nonaqueous Battery Systems

Lithium has the lowest equivalent weight among all the alkaline metals and the largest negative potential. Therefore, when used as the negative electrode in batteries, it offers a very high energy density. Within the last ten years considerable effort has been devoted to the development of nonaqueous batteries in order to exploit fully the advantages of lithium as a negative electrode. Two types of nonaqueous batteries are being developed, high temperature and room temperature systems. The high temperature systems use molten salt as electrolyte thus avoiding the need for a nonaqueous solvent. The Li-FeS₂ battery using molten LiCl-KCl eutectic as the electrolyte is an example, and a great deal of effort has been expended in its development (1-4). A large proportion of development work in room temperature systems has been directed towards finding a positive electrode and an electrolytic solution compatible with the lithium negative electrode. For a feasible battery system, the solvent must be stable with lithium, the electrolyte must be compatible with both the solvent and lithium, the electrolytic solution must have a conductivity of at least $10^{-3} \text{ ohms}^{-1} \text{ cm}^{-1}$, and the positive electrode while being compatible with the electrolytic solution must contain an active material that is sufficiently insoluble in the solvent so that self-discharge is minimized.

Several lithium battery systems, primary as well as secondary, have been reported in the literature (5-23). These are listed in Table 1-A and 1-B to illustrate the diversity in the search for a suitable

TABLE 1. ROOM TEMPERATURE NONAQUEOUS BATTERY SYSTEMS USING LITHIUM NEGATIVE ELECTRODES

A. PRIMARY SYSTEMS

ELECTROLYTE	SOLVENT	POSITIVE ELECTRODE	YEAR	REF
1. LiClO ₄	THF + DME	CuS on Nickel plated steel	1969	5, 12
2. LiClO ₄	DMSU or PC	(CF _x) _n + Acetyline black on nickel	1970	13, 16
3. LiClO ₄	EC	CuF ₂ + Graphite on copper	1971	8
4. LiBF ₄ or LiBr or LiPF ₆	SL or DMSO	Graphite (rod)	1971	9
5. LiAlCl ₄ or LiAsF ₆	BL	MoO ₃ + Graphite on copper	1971	11, 20
6. LiAsF ₆	PC	CF + Graphite on copper	1973	13
7. LiClO ₄	PC	MnO ₂ + Graphite on copper	1973	13, 18
8. LiClO ₄	PC	C _x O _y H _z + Graphite on copper	1973	13
9. LiClO ₄	DMF	MeBS + Graphite* on copper	1973	14
10. LiAlX ₄ or LiBX ₄	POCl ₃	X on Carbon	1973	15
11. LiAlCl ₄	POCl ₃	Me +	1973	15
12. LiBCl ₄	POCl ₃ , SOCl ₂	CuF ₂ or (CF) _n or WO ₃ or S + graphite on copper.	1973	15, 16
13. LiClO ₄	PC or THF + DME	MoO ₃ or MnO ₂ + graphite on nickel	1974	18
14. LiAsF ₆ or LiClO ₄	MF, BL or THF + DME	Ag ₃ PO ₄ or Ag ₃ AsO ₄ or Ag ₂ CrO ₄	1975	22
15. LiAlCl ₄	BL	MoO _n or WO _n (2.5 ≤ n ≤ 3) + graphite on copper	1975	23

Abbreviations used in the table are explained at the end of part B.

B. SECONDARY SYSTEM

ELECTROLYTE	SOLVENT	POSITIVE ELECTRODE	YEAR	REF
1. LiAlCl_4	MCC	Cu_2Cl_2 or CuCl_2 on Nickel plated steel	1969	5
2. LiClO_4 or LiBF_4	DMSU or PC	Graphite (thin plates)	1971	10
3. LiClO_4 + LiBr	PC	Br_2 on Carbon	1974	17
4. LiClO_4	THF + DME	MnO_2 + graphite on Nickel	1974	18
5. LiAlCl_4	PC	NbS_3 on Nb	1974	19
6. LiAlCl_4 or LiClO_4 or LiBF_4	PC	TiS_2 or TiS_3 on Ti	1975	21

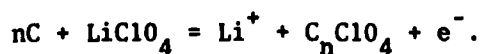
Abbreviations used for solvents:

BL = γ - Butyrolactone	MCC = Methyl chlorocarbonate
DME = 1, 2 - Dimethoxyethane	MF = Methyl formate
DMF = Dimethyl formamide	PC = Propylene carbonate
DMSU = Dimethyl sulfite	SL = Sulfolane
DMSO = Dimethyl sulfoxide	THF = Tetrahydrofuran
EC = Ethylene carbonate	
*MeBS - Metallic borosulfides - CuBS, AgBS, $\text{Pb}_2\text{B}_2\text{S}_5$, $\text{Mn}_2\text{B}_2\text{S}_4$	
†Me - Metal - Pb, Ta, Ti, W, Nb, Pd, Ag, Fe, Mn, Mo, Co, SS, Ni, Pt, Hg, Au	

combination of a positive electrode and an electrolytic solution for a nonaqueous lithium battery system. The stability and performance of the lithium negative electrode in a wide variety of solvents has been studied (24-28). It has been shown that the water content in electrolytic solutions must be less than 50 ppm (24, 26). The mossy dendritic nature of lithium deposits and the apparent reaction with the solvent (28) are problems that must be overcome to use lithium successfully in a rechargeable battery. Secondary batteries need thin, ion-exchange membranes as separators. Although separators are essential in the battery, no work directed towards selecting a membrane specifically suited to lithium batteries has been reported in the literature.

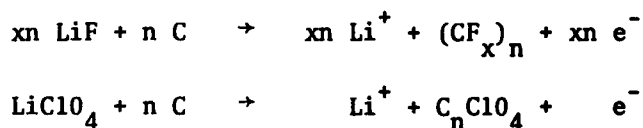
Lithium-Graphite Battery

The lithium-graphite battery system using LiClO_4 -Dimethylsulfite (DMSU) as the electrolytic solution is the focus of this thesis. The behavior of DMSU as a battery solvent was studied (29) and the transport properties of LiClO_4 in DMSU were measured (30) before the battery system was investigated (10). The feasibility of the cell $\text{Li}/\text{LiClO}_4, \text{DMSU}/\text{Graphite}$, capable of delivering up to 10 mA/cm^2 at 4.0 V has been demonstrated. Maximum charge storage of 90 coulombs/g of graphite with up to 90% coulombic efficiency was achieved. No significant differences were found upon substituting the electrolyte and the solvent. On wet stand, the cells retained 50 to 75% of their capacity. On the basis of these results, it was proposed that a simple lamellar compound of graphite is formed in the LiClO_4 -DMSU solutions, characterized by the reaction



If this were the stoichiometry, the charge storage capacity of 90 coulombs/g of graphite corresponds to 89 carbon atoms per ClO_4^- anion. The corresponding specific energy density for the battery was predicted to be 20-45 Wh/Kg at a 4.0 V discharge potential, assuming graphite constitutes 20% of the weight of the battery.

The weight of the anion and the number of carbon atoms required per anion are important parameters in calculating the specific energy density. Both must be lowered to increase the energy density. Hebbbar (31) attempted intercalation of the light fluoride ion and demonstrated charge storage capacities of over 3000 coulombs/g of graphite with 100% coulombic efficiency above 3.0 V potential (measured with respect to a lithium wire reference electrode). Two discharge plateaus were observed, one above 4.2 V characteristic of perchlorate intercalation (10) and the other above 3.0 V typical of Li/CF_x primary batteries (6, 7). Two reactions have been suggested.



Since both reactions involve only one electron being transferred, the charge storage capacity of 3000 coulombs/g of graphite implies that less than 3 carbon atoms are required per anion intercalated. Another implication is that the specific energy density can be projected to be 250 Wh/Kg at a 3.0 V discharge potential if graphite is assumed to constitute 10% of the weight of the battery.

Hebbbar did not investigate the possible role of the solvent in the cell reactions. The exact stoichiometry of the intercalation was not determined. With a view to ascertaining the exact nature of cell reactions

and the involvement of the solvent (DMSU) and the electrolyte (LiClO_4), they were substituted with an alternate solvent (propylene carbonate-PC) and an alternate electrolyte (lithium tetrafluoroborate- LiBF_4) in successive experiments of this study. Possible specificity of cell performance to LiF or graphite used in the positive electrode was investigated by not using one or both of these components in some experiments. Experiments were performed to determine the maximum operating current density and establish the feasibility of using thin electrodes. Electrode thickness and operating current density are important parameters of the power density of a battery. Hebbbar (31) had shown that the charge recovered at the 3.0 V plateau was at least fifteen times as large as the 4.0 V plateau. Results of Dunning et al (10), based on the higher plateau, were therefore reexamined with the focus on the 3.0 V plateau and the possible participation of solvent in the reactions occurring in the cell during cycling.

Chapter 2

EXPERIMENTAL

Materials

Dimethylsulfite (DMSU) and propylene carbonate (PC) were the aprotic solvents used. DMSU was purchased from Pacific Chemical Company, Hawthorne, California. It was vacuum distilled in the apparatus described by Tiedemann (32) to reduce its water content to less than 50 ppm as determined by the Karl Fischer technique. PC was supplied by Eastern Organic Chemicals, Rochester, New York, and was used as received. Both solvents were stirred with lithium chips for 48 to 72 hours and filtered before using them to prepare solutions.

Lithium perchlorate (LiClO_4) and lithium tetrafluoroborate (LiBF_4) were used as electrolytes. Pure LiClO_4 purchased from K and K Labs, Irvine, California was vacuum dried just below the melting point (235°C) at 40 μHg pressure. Batches of 25-30 g of LiClO_4 each were dried and ground in a petri dish three or four times. Ultrapure LiClO_4 received from Anderson Physics Labs, Urbana, Illinois was used as received. LiBF_4 supplied by Foote Mineral Company, Exton, Pennsylvania was repeatedly heated in vacuo at 120°C and 50 μHg for six hours and powdered until the salt remained free flowing at the end of vacuum heating.

Lithium ribbon used for the negative as well as the reference electrodes was supplied by the Foote Mineral Company, Exton, Pennsylvania. The ribbon was 5 cm wide and 0.4 mm thick. It was packed in dry Argon gas.

Purified graphite powder (99.95% pure, 0.8 μ in size) made from natural Madagascar graphite was used for forming positive electrodes.

It was received from Asbury Graphite Mills Inc., Oakland, California.

Lithium fluoride (LiF) tested as an additive to the positive electrode was acquired from J. T. Baker Co., Philipsberg, New Jersey. LiF was vacuum dried at 800°C and 50 μ Hg for six hours.

Graphite glue and teflon moulding powder were used as binders in the preparation of the positive electrodes. Union Carbide Carbon Products Division, New York, New York supplied National C-34 graphite glue. The glue comes in two parts; a fine black powder and a dark liquid, which must be used together. Teflon moulding powder was acquired from Liquid Nitrogen Processing Corporation, Santa Ana, California. It is a fine (200 mesh) white powder.

Carbon Cloth and titanium foil were used as current collectors. Carbon cloth was received from Union Carbide Carbon Products Division, New York, New York. It is also called graphite cloth because it is prepared by graphitising a woven fabric. The cloth is 0.2 to 0.4 mm thick. It was treated with acetone in a Soxhlet extractor before use. Titanium foil, 0.03 mm thick was purchased from Teledyne Rodney Metals, Pico Rivera, California.

Apparatus

All experiments were performed in a dry box supplied by Vacuum/Atmospheres Corporation. Hebarr (31) has described the dry box in detail. Since then, a vacuum oven, Model VT 13-24-6, has been added. This oven, attached to the dry box, is a fully water-jacketed, stainless steel vacuum vessel with internally mounted radiant heaters and stainless steel reflectors. It can be heated up to 600°C and evacuated down to 50 μ Hg. The oven is used for outgassing and drying. It is equipped

with a proportional temperature controller and temperature and pressure gages. Drying of electrolytic salts and preparation of the electrolytic solution are carried out inside the dry box.

Experiments were performed in H-cells because such a cell design helped isolate the positive and negative electrodes, along with their respective solutions. All changes occurring at the two electrodes could be observed continuously, clearly and separately in this cell configuration. The H-cell, shown in Figure 1, has two vessels, each 2.5 cm in diameter, connected by a limb 1.25 cm in diameter. Isolation of the two compartments is achieved by a Corning fine size (5μ pores) glass frit mounted in the middle of the connecting limb. Two polyethylene stoppers were used to minimize the solvent losses by evaporation. All electrode leads were drawn out from the top, between the stopper and the glass well. Consequently the stoppers did not provide a hermetic seal. The two electrodes were held down flat at the bottom of the two compartments by glass sleeves 2 cm in diameter and 1.25 cm high. The sleeves were designed so as not to block the current path through the connecting limb. When the cell was filled, the liquid surface was kept just above the connecting limb; each vessel of the H-cell contains about 10 cc of solution at that level.

Figure 2 shows the electrical circuit in which the cell was charged and discharged. The circuit consisted of a power source (two lead acid batteries in series), a variable resistance box, Heathkit Model IN-11, an ammeter, Simpson Model 260 Volt-ohm-millammeter, and a digital coulometer, Koslow Scientific Company Model 541, all connected in series with the experimental cell. An electrometer, Keithley Model 610 B, was

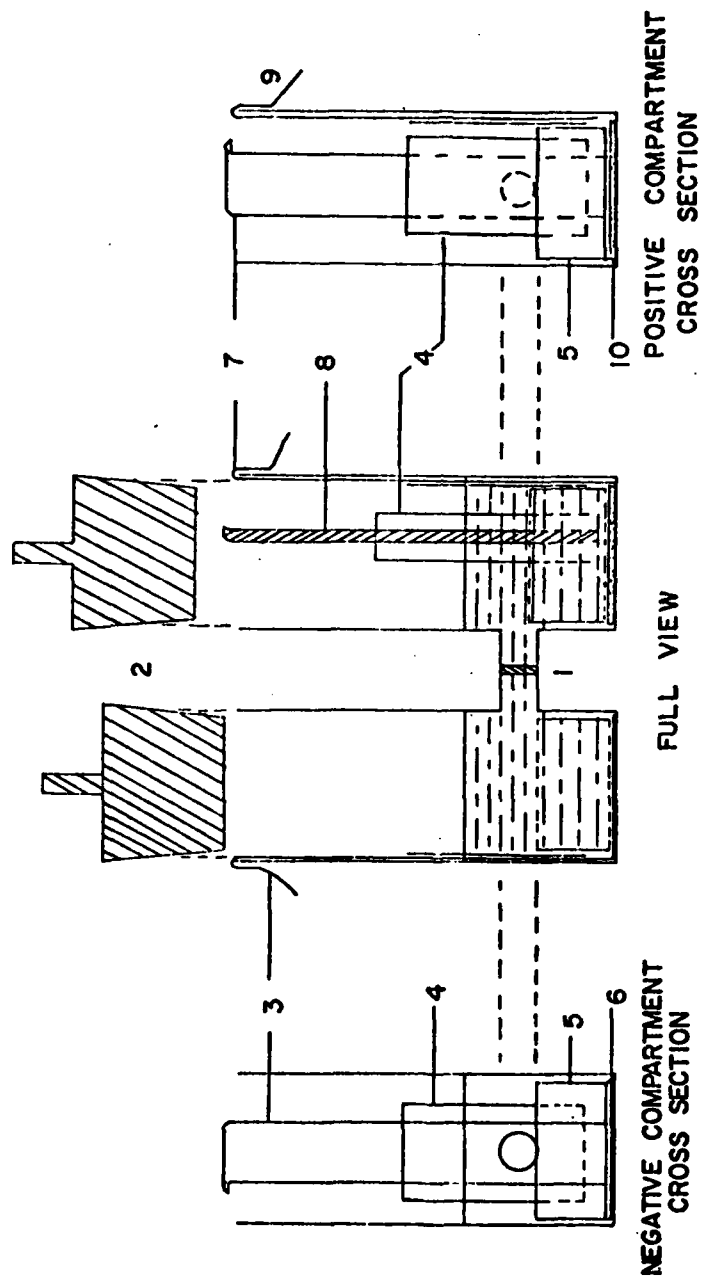


Figure 1. The H-cell used in all experiments.

Legend: 1: Glass Frit. 2: Polyethylene stoppers. 3: Negative lead. 4: Polypropylene masks for the three electrodes. 5: Glass sleeve. 6: Negative electrode. 7: Positive lead. 8: Reference electrode. 9: Reference lead. 10: Positive electrode.

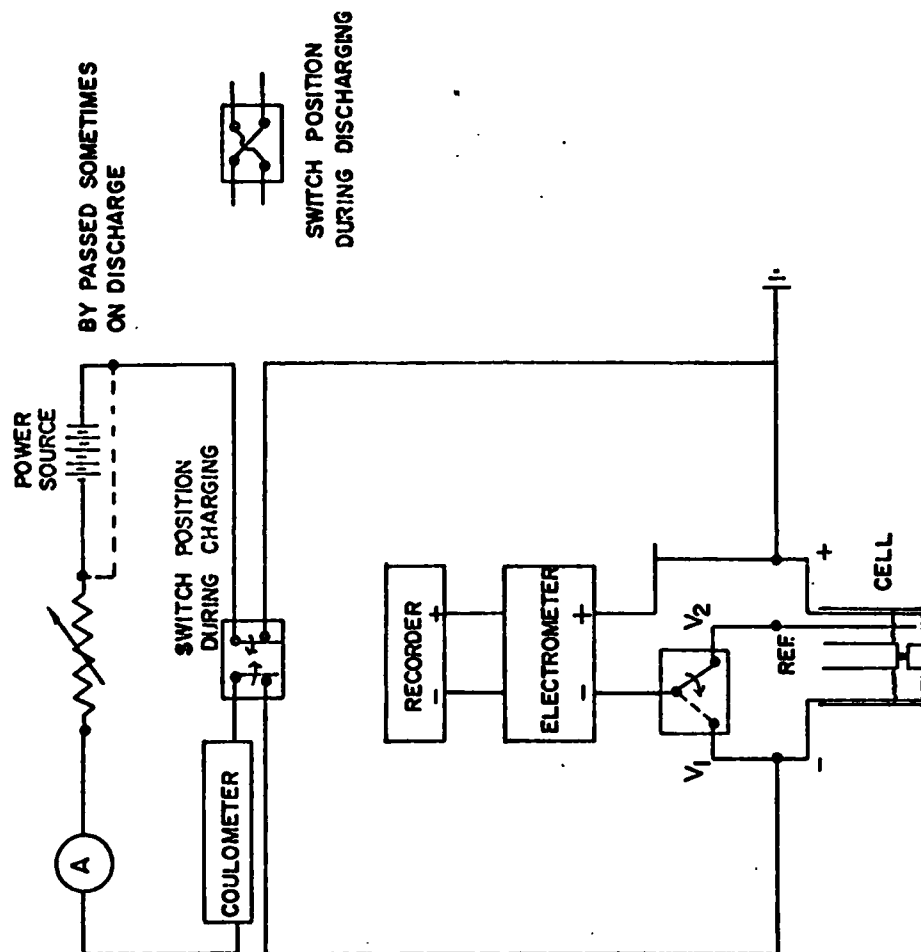


Figure 2. Electrical circuit diagram for charging and discharging.

connected in parallel to the cell for potential measurements. The measured potentials were recorded on a Sargent recorder, Model SR. During discharge on some runs, the cell was not driven by the batteries, which were bypassed as shown by dotted lines in Figure 2.

X-ray powder diffraction patterns were obtained on the Norelco X-ray diffractometer using Cu radiation and a Ni filter. Perkin Elmer spectrophotometer, Model 421, was used for IR analysis and Perkin Elmer chromatograph, Model 880, provided with a hot wire detector accessory, Model 800, was used for chromatographic analysis of the solution.

Preparation of positive electrodes

Positive electrodes of three types were tested: pyrolyzed, pressed, and cloth electrodes.

Pyrolyzed electrodes were made using the graphite glue. The powder part of the glue was intimately mixed with twice its weight of graphite. In one electrode no graphite was added whereas in another LiF was added to the mixture of graphite and glue. The other part of the glue, the dark liquid, was added to the mixture to form a viscous paste. The paste was then spread on the carbon cloth and pressed between two steel plates to form a disk 1 mm or less thick. The disk, still held between the steel plates, was fired in an inert atmosphere of pure Argon at 800°C for at least six hours. The electrode was pyrolyzed to a solid, brittle, porous disk adhering very well to the carbon cloth. The disc separates easily from the confining steel plates. The resistance of these electrodes was generally around 5 ohms. The surface was rough and dull.

The pressed electrodes contained teflon moulding powder as the

binder. They were formed by intimately mixing equal weights of graphite and the moulding powder and hot pressing the mixture on to the carbon cloth or perforated titanium foil used as the current conductor. Hot pressing was performed with a hydraulic press at 8000 psi and 100°C. The electrode thus formed was a solid, fragile, porous disk, less than 1 mm thick. Adherence to titanium was satisfactory but was poor in the case of carbon cloth. Predictably, the electrode with titanium backing plate had a smaller resistance (5 ohms) than the carbon cloth backed electrode (8 ohms). The teflon in the electrodes is considered inert. The electrode surface was smooth and shiny.

Carbon cloth used as a current collector in the other two types of electrode, was used as the positive electrode by itself. Strips of the cloth washed with freshly distilled acetone were used.

Assembling the cell

Cells were always assembled in the discharged state. The positive electrode, prepared as above, was placed in the H-cell and dried under vacuum, at 50 μ Hg and 120°C, for six hours in the vacuum oven attached to the dry box. A thin strip of lithium was inserted as the reference electrode in the compartment that contained the positive electrode. In the other compartment, a lithium strip (0.5 cm wide), with a circle (2.5 cm in diameter) attached at one end, was inserted such that the circle covered the bottom of the compartment; this was the negative electrode. Glass sleeves were slipped into each compartment to hold the electrodes down. The cell was then filled with the electrolytic solution until the connecting limb was just submerged fully. Gas bubbles trapped under the electrodes and between electrode leads, glass

sleeve and the wall were shaken free. Strips of polypropylene sheet were slipped over all electrode leads to prevent a direct path to them for the current. Thus, the current was forced to take the path from the bottom of one compartment to the other through the glass frit.

Charging and discharging

Galvanostatic charging and discharging was accomplished in the electrical circuit shown. Various coulombic extents (time periods) and rates of charging were used. The open circuit potential was observed, and the measured potentials were recorded versus time during both charging and discharging.

Generally, the cycled cells were of the type

Li/LiClO₄, DMSU/Graphite positive electrode

but some components were substituted. Propylene carbonate was another solvent used and LiBF₄ the substitute electrolyte. Carbon cloth and titanium were used as the current collector at the positive electrode. In one experiment LiF was used as an additive in the graphite positive electrode while in another an electrode containing only graphite glue on carbon cloth was used. In a pair of experiments, the positive electrode consisted of either carbon cloth or platinum foil by itself. In all experiments lithium was used as the substrate for lithium deposition at the negative electrode.

Chapter 3

RESULTS

Measurements and Observations

Preliminary experiments were performed to study the structural changes occurring in pyrolyzed (containing graphite glue as binder) and pressed (bonded by teflon moulding powder) graphite positive electrodes upon repeated cycling, and, to select the structurally more stable electrode of the two. In another experiment, the effectiveness of LiF as a positive electrode additive was tested. The main study was intended to demonstrate the reversible electrical storage capacity of the Li/LiClO₄, DMSU/Graphite battery system and to determine the effect of charging and discharging rates (current) on the performance of this battery system. In addition, specificity of the observed performance to the solvent, the electrolyte, the graphite, and the backing material used in the positive electrode was examined by replacing each one of them in turn in successive experiments. Infra red, X-ray powder diffraction, and chromatographic analyses were performed on samples from cycled cells to identify the products of the charging and discharging reaction.

The data gathered from the various experiments consisted of the following observations and measurements: 1) The open circuit potential of the cell when assembled or 30 seconds after an interruption in charging or discharging, denoted by V_0 ; 2) The open circuit potential of the cell after several hours of interruption in charging or discharging, called the wet stand potential and denoted by V'_0 ; 3) The cell potential during charging or discharging, measured as the potential of a lithium negative electrode versus the positive electrode and denoted by V_1 ;

4) The potential of a lithium wire reference electrode located as shown in Figure 1 versus the positive electrode, denoted by V_2 ; 5) The charge stored in the cell during charging, denoted by Q_{in} ; 6) The charge recovered from the cell with V_2 above 4.0 V, denoted by Q_{4V} ; 7) The charge recovered from the cell above the cut-off voltage, V_f , denoted by Q_{V_f} (includes Q_{4V}); 8) The operating current, denoted by I ; and 9) The resistance of the positive electrode measured between a point on the porous disc and a point at the end of the electrode lead.

All or some of the above are included in the results. All potential measurements were made with the positive electrode of the cell grounded. The measured values have been multiplied by -1 and then reported, so that the reported values conform to the usual sign convention.

Results for all experiments are presented in the form of charge-discharge characteristics. Both charging and discharging were galvanostatic. Charge-discharge characteristics are plots of the observed values of V_2 for corresponding values of the charge stored during charging (Q_{in}) or the charge recovered during discharging (Q_{V_f}). While V_2 is expressed in milliequivalents (mEq or 10^{-3} Eq). Values of V_0 and V_0' are also plotted along with these characteristics.

Discharge runs were terminated in most cases when V_2 reached the predetermined cut-off potential, V_f , selected to be lower than the open circuit potential of the cell when assembled. Sometimes discharge was continued until V_2 exhibited a rapid drop.

Preliminary experiments

Electrodes prepared by two different techniques, pyrolyzing and

pressing, were tested for structural stability after repeated cycling in the cells of the type Li/LiClO_4 , DMSU/Graphite positive electrode. Figure 3 shows the typical charge-discharge characteristics for cell 1 containing a pyrolyzed graphite positive electrode whereas Figure 4 shows those for cell 2 containing a pressed graphite positive electrode. It is seen that for both the cells charging occurred with V_2 at 4.90 V and discharging with V_2 at 3.00 V. Reversible charge storage in both cells was in the 2 to 3 mEq range with 100% coulombic efficiency above $V_f = 2.50$ V. Both pyrolyzed electrodes swelled during the charging run of the initial two or three cycles. The pyrolyzed electrode remained rigid and hard. The adherence of the porous carbon disk to the carbon cloth (backing material) was good, after six cycles. The pressed electrode, on the other hand, was very soft at the end of five cycles. Adherence of the porous disk to the carbon cloth was poor to start with. Thus, the pyrolyzed electrode appeared to be structurally more stable than the pressed electrode on repeated cycling.

Carbon cloth was used as the current collector in the above experiments. The carbon cloth showed no signs of being chemically changed after repeated cycling. But, carbon cloth is an unlikely choice for current collector in commercial applications, because it shreds easily and has no rigidity. These mechanical shortcomings can be avoided by using a metallic current collector. Hebbar (31) successfully used platinum as current collector in his test cells. However, the prohibitive cost of platinum precludes its use in actual commercial batteries. Titanium was tested as a possible current collector. A positive electrode prepared by pressing a mixture of graphite and teflon moulding

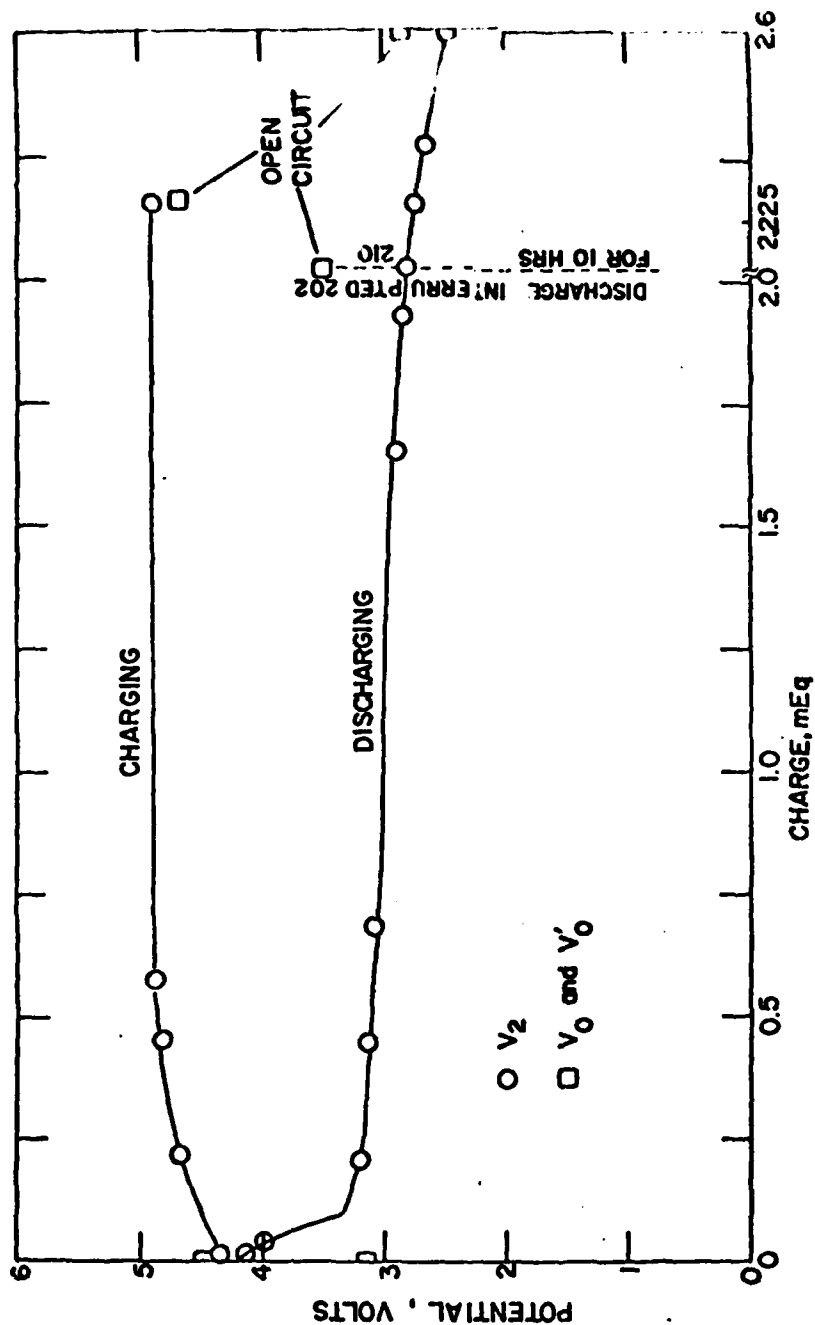


Figure 3. Typical galvanostatic charge-discharge curves for the cell Li/LiClO_4 , DMSO (1.0M)/Graphite + Graphite glue on Carbon cloth. Cycle No. 3. $I = 5.0 \text{ mA}$. $Q_{\text{th}} = 2.274 \text{ mEq}$. Coulombic Eff. = 114.4% above $V_f = 2.45\text{V}$. Positive Electrode weight = 0.5468g. Graphite = 0.1040g. Carbon cloth = 0.3893g. Initial thickness of carbon disc. = 0.0686 cm. Top surface area = 3.14 cm^2 . Resistance = 5.0 ohms.

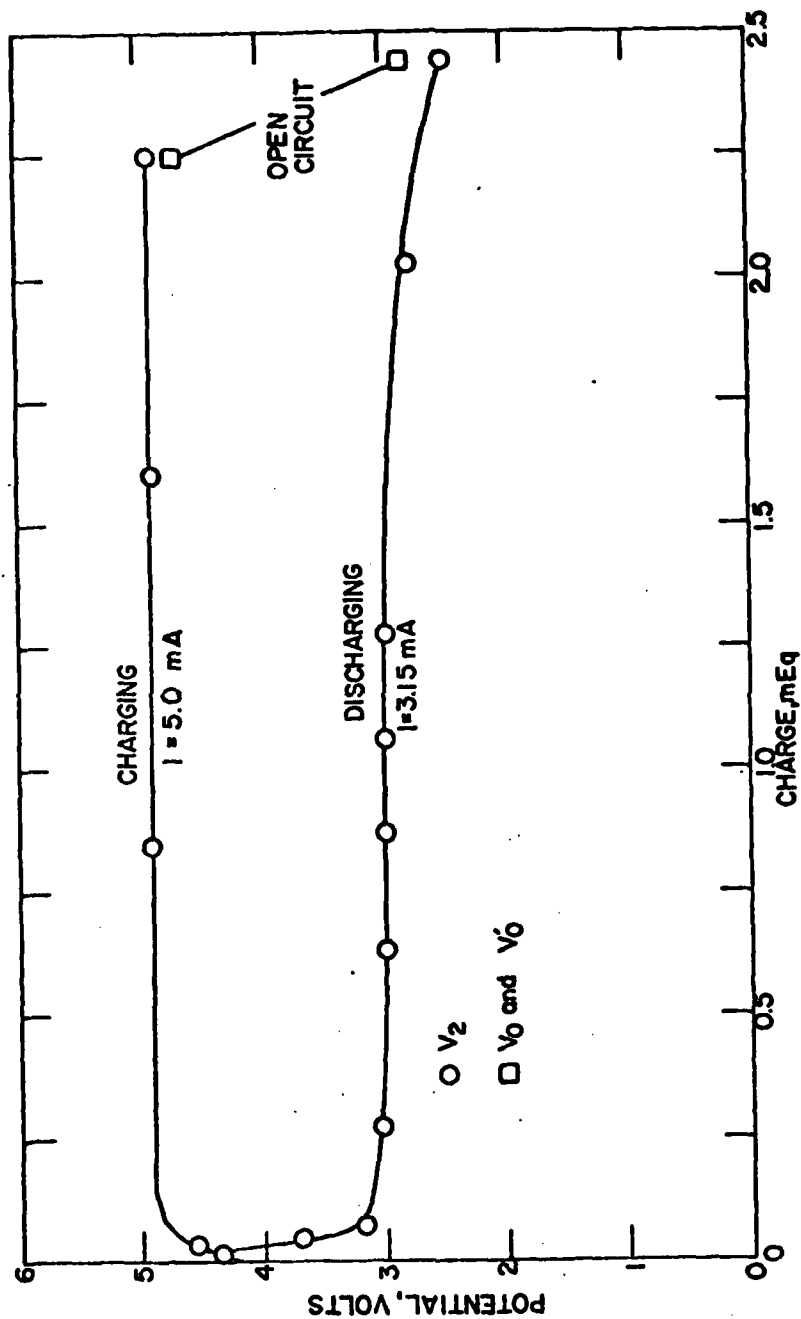


Figure 4. Typical galvanostatic charge-discharge curves for the cell Li/LiClO_4 , DMSU (1.0M) Graphite + Teflon powder on carbon cloth. Cycle No. 3. $I = 5.0, 3.15 \text{ mA}$. $Q_{in} = 2.22 \text{ mEq}$. Coulombic Eff. = 109.9% above $V_f = 2.50 \text{ V}$. Positive electrode weight = 0.8268g. Graphite = 0.1654g. Carbon cloth = 0.5000g. Initial thickness of carbon disc = 0.1200 cm. Top surface area = 3.14 cm^2 . Resistance = 8.00 ohms.

powder on two sides of perforated titanium foil was used for the purpose. In the first cycle (Figure 5) the cell (cell 2a) charged at a high potential ($V_2=5.45$ V compared to $V_2=4.90$ V when carbon cloth was used). On discharge the potential (V_2) dropped rapidly. When V_2 was at 2.00 V, only 0.07 mEq had been recovered which meant a coulombic efficiency of 20%. Within 24 hours of assembling the cell and before the next cycle could be started, the titanium lead from the positive electrode was found to have corroded away. The inability of titanium to remain chemically inert in the cell, coupled with the poor performance of the positive electrode containing titanium, was considered evidence that titanium is unsuitable as current collector in the battery system being investigated. Therefore, carbon cloth was used as the current collector in all later experiments.

Improvement in the reversible electrical storage of the battery upon use in LiF in the positive electrode was tested in another experiment. A cell (cell 1a) with a pyrolyzed graphite positive electrode containing LiF was cycled. Typical charge-discharge characteristics are shown in Figure 6. Charging and discharging plateaus are almost the same as those in Figure 3 and 4. One difference is the longer upper plateau ($V_2>4.00$ V) in Figure 6, which represents the fourth charge-discharge cycle. On earlier cycles this plateau was even longer, but on later cycles it was not observed. Therefore, the 4.00 V plateau is not considered a significant difference. On the whole, the fact that the charging and discharging potentials were the same in the presence or absence of LiF, suggests that the involvement of LiF in the positive half-cell reactions and its (LiF) contribution to battery performance

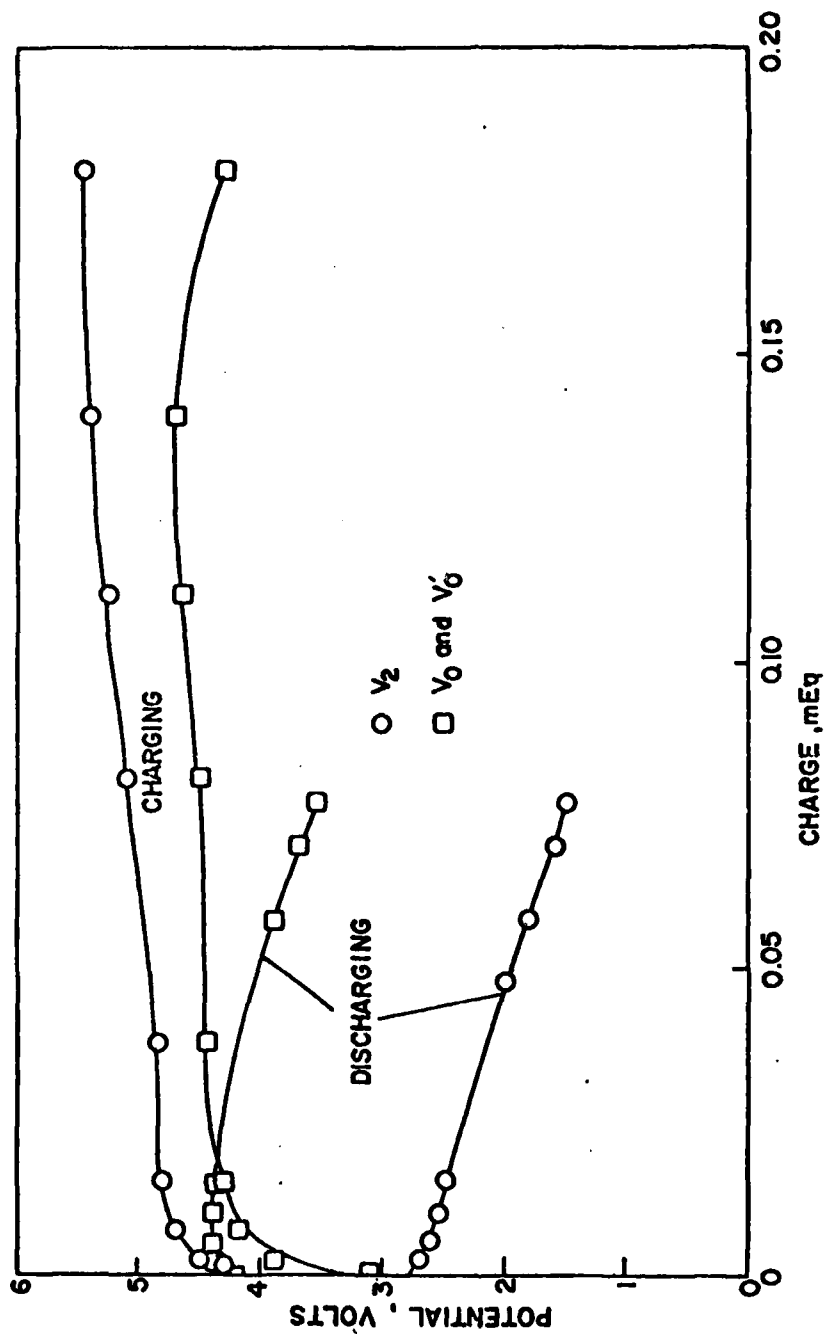


Figure 5. Galvanostatic charge-discharge curves for the cell Li/LiClO₄, DMSU (1.04M) Graphite + Teflon powder on titanium. Cycle No. 1. $I = 3.15$ mA. $Q_{in} = 0.18$ mEq. Coulombic Eff. = 27.2% above $V_f = 2.00$ V. Positive electrode weight = 0.4373g. Graphite = 0.1857g. Titanium = 0.0704g. Initial thickness of carbon disc = 0.05 cm. Top surface area = 3.14 cm². Resistance = 5.00 ohms.

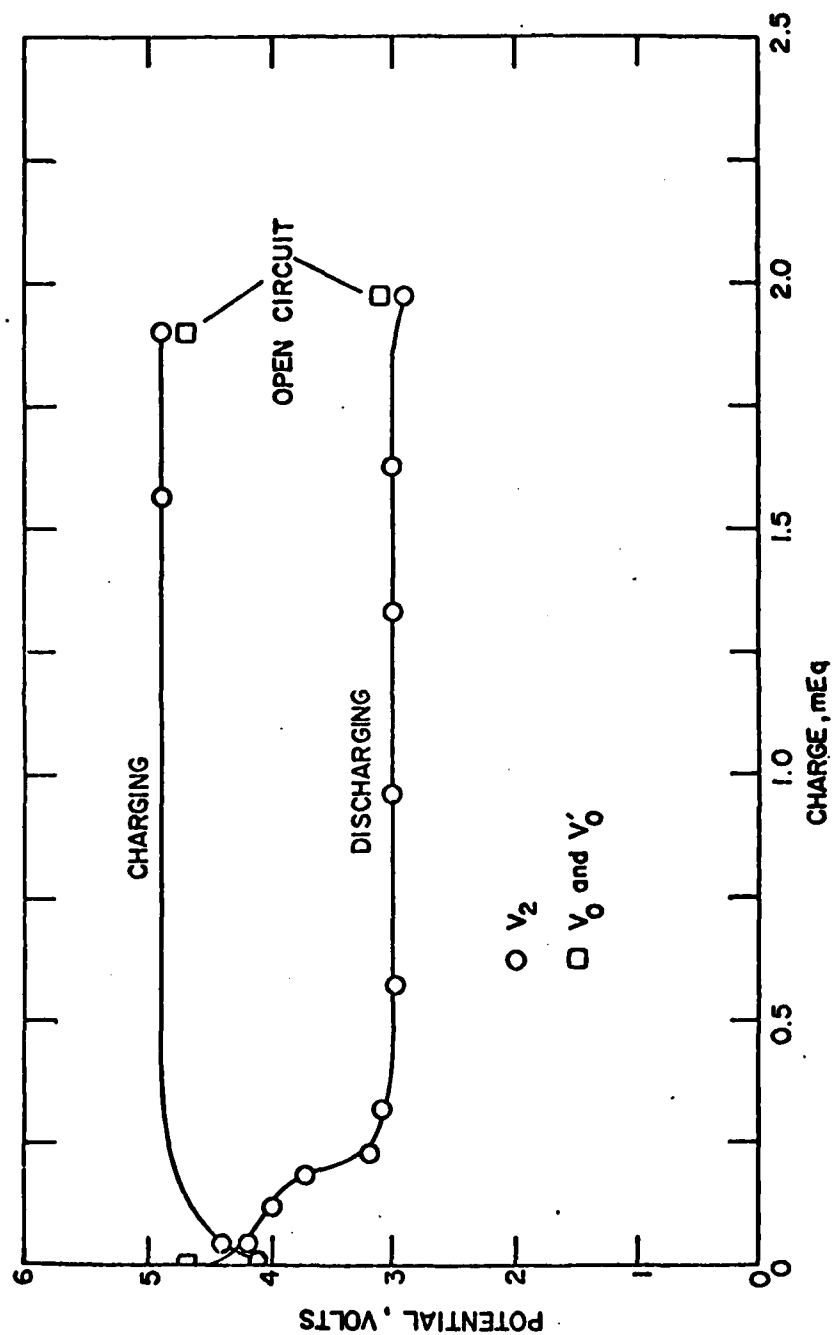


Figure 6. Typical galvanostatic charge-discharge curves for the cell Li/LiClO₄, DMSU (1.0M)/Graphite + LiF + Graphite glue on Carbon cloth. Cycle No. 4. $I = 4.50$ mA. $Q_{in} = 1.90$ mEq. Coulombic Eff. = 103.6% above $V_f = 2.90$ V. Positive electrode weight = 0.5010g. Graphite = 0.1153g. Carbon cloth = 0.2510g. LiF = 0.0784g. Initial thickness of carbon disc = 0.10 cm. Top surface area = 3.14 cm². Resistance = 5.0 ohms.

is negligible.

Performance of the Li/LiClO₄, DMSU/Graphite Battery System

I. Demonstration of reversible electrical storage capacity:

Data from charge-discharge cycles

In this experiment, the positive electrode was of the pyrolyzed graphite type. The electrode weighed 0.7245 g of which the carbon cloth constituted 0.3735 g and graphite 0.2318 g, the rest being pyrolyzed graphite glue. Initial thickness of the electrode was 1 mm and the diameter 2.0 cm. The electrode had a resistance of 1.0 Ohm. The LiClO₄-DMSU solution filled in the cell contained 1.04 moles LiClO₄/1000 ml of solution. When the cell was filled, its open circuit potential, V_0 , was 2.70 V.

The cell was cycled four times. On each cycle, a larger amount of charge was stored than on the previous cycle. The charge-discharge characteristics for the four cycles are shown in Figures 7, 8, 9 and 10. Charging and discharging was carried out at 3.20 mA (1 mA/cm²) on the first cycle and 6.3 mA (2 mA/cm²) on cycles 2, 3 and 4. On cycle 2 current was increased to 10 mA for short intervals.

Charging runs on all four cycles exhibited very flat plateaus. On the first cycle V_2 attained its peak value, 4.83 V, gradually. On later cycles, with a higher current, the peak value was attained quickly. Typically, the V_0 curve is parallel to the V_2 curve except at the beginning of the charging run. The difference $V_2 - V_0$ represents the overpotential at the positive electrode during charging. This overpotential was smaller on the first cycle because of the lower current.

Discharging was started immediately after charging was stopped on

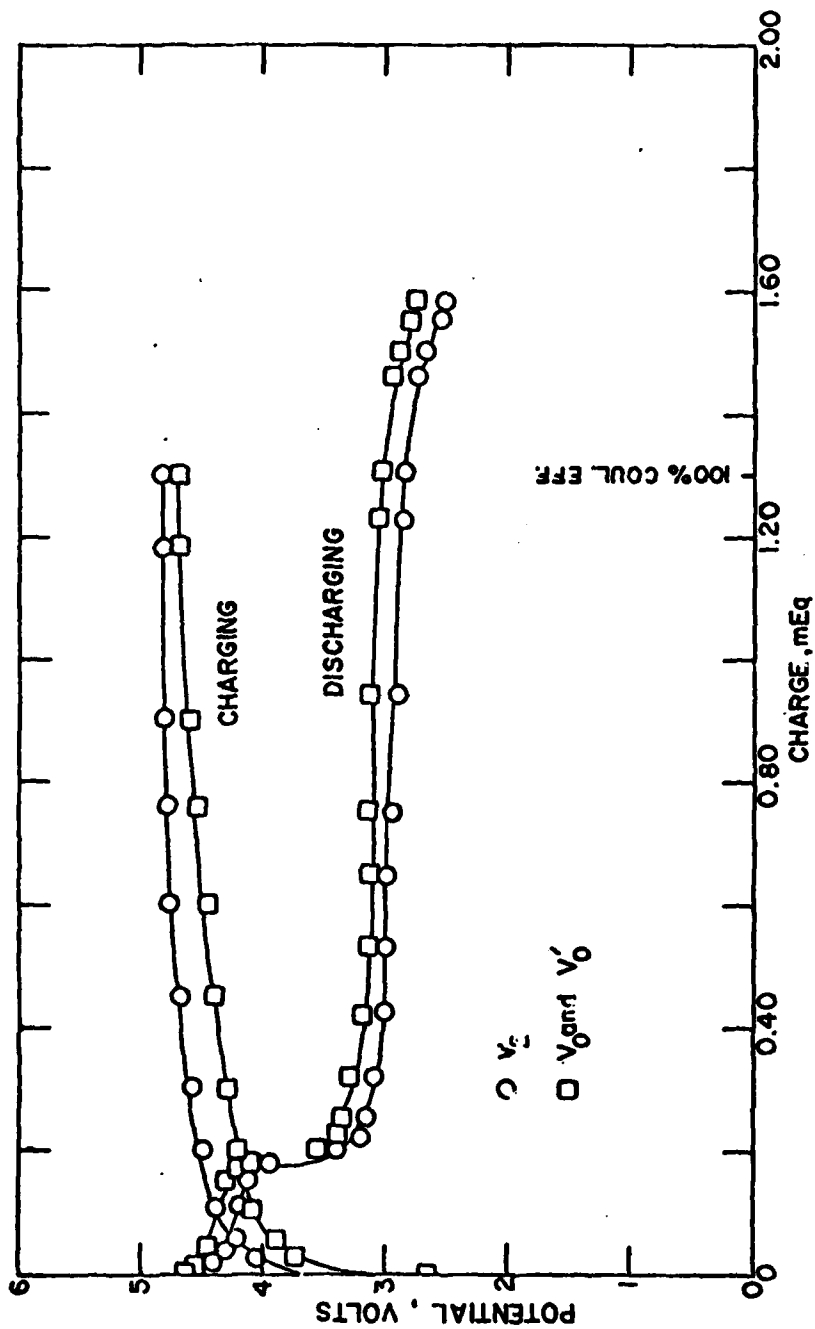


Figure 7. Galvanostatic charge-discharge curves for the cell Li/LiClO_4 , DMSU (1.0M)/Graphite + Graphite glue on Carbon cloth. Cycle No. 1. $I = 3.20 \text{ mA}$. $Q_{in} = 1.30 \text{ mEq}$. Coulombic Eff. = 121.5% above $V_f = 2.50\text{V}$. Discharge begun after 0 hours of wet stand on charge. Positive electrode weight = .7245g. Graphite = 0.2318g. Carbon cloth = 0.3735g. Initial thickness of carbon disc = 0.1 cm. Top surface area = 3.14 cm^2 . Resistance = 1.0 ohm .

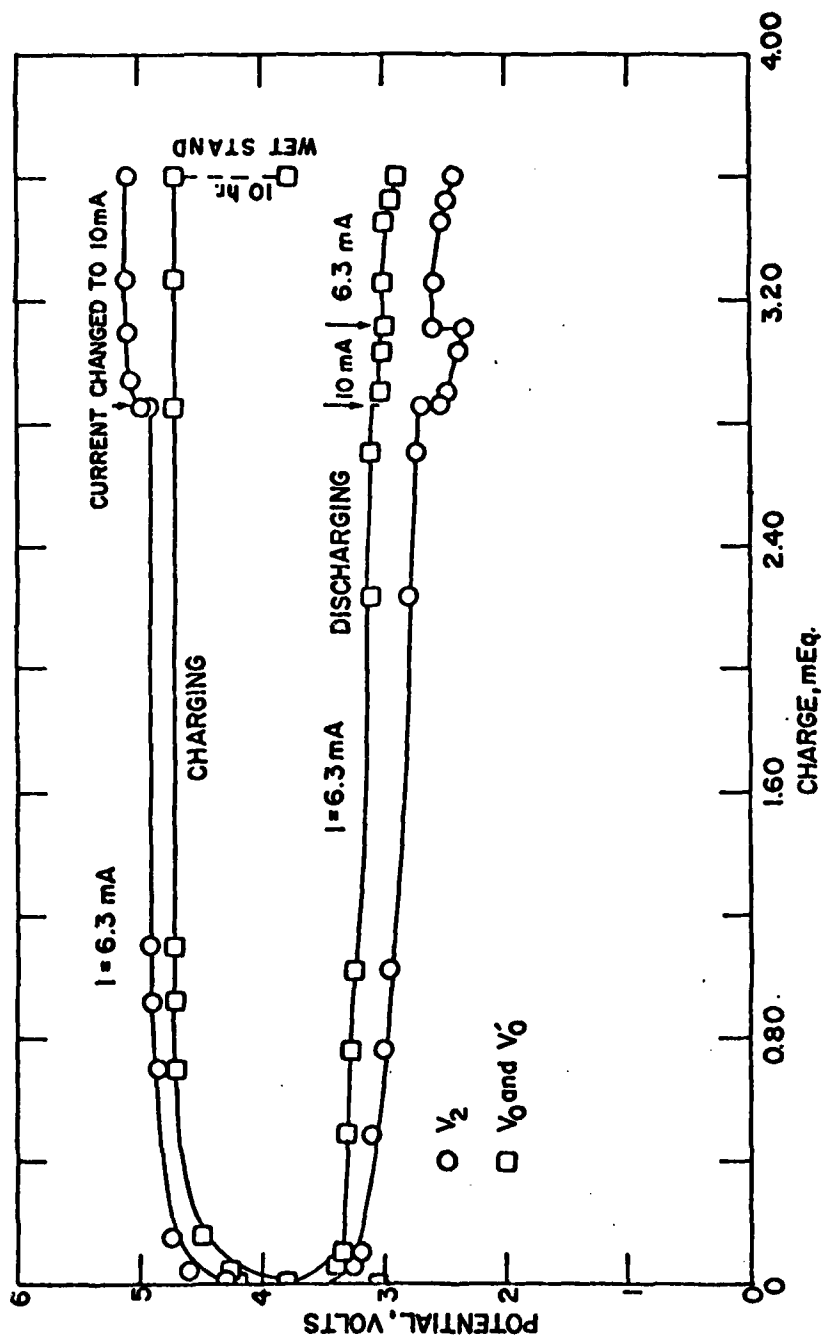


Figure 8. Galvanostatic charge-discharge curves for the cell Li/LiClO_4 , DMSU (1.0M)/Graphite + Graphite glue on Carbon cloth. Cycle No. 2. $I = 6.30 \text{ mA}$. $Q_{in} = 3.60 \text{ mEq}$. Coulombic Eff. = 100.0% above $V_f = 2.50 \text{ V}$. Discharge begun after 10 hours of wet stand on charge. Positive electrode weight = .7245g. Graphite = 0.2318g. Carbon cloth = 0.3735g. Initial thickness of carbon disc = 0.1 cm. Top surface area = 3.14 cm^2 . Resistance = 1.0 ohm .

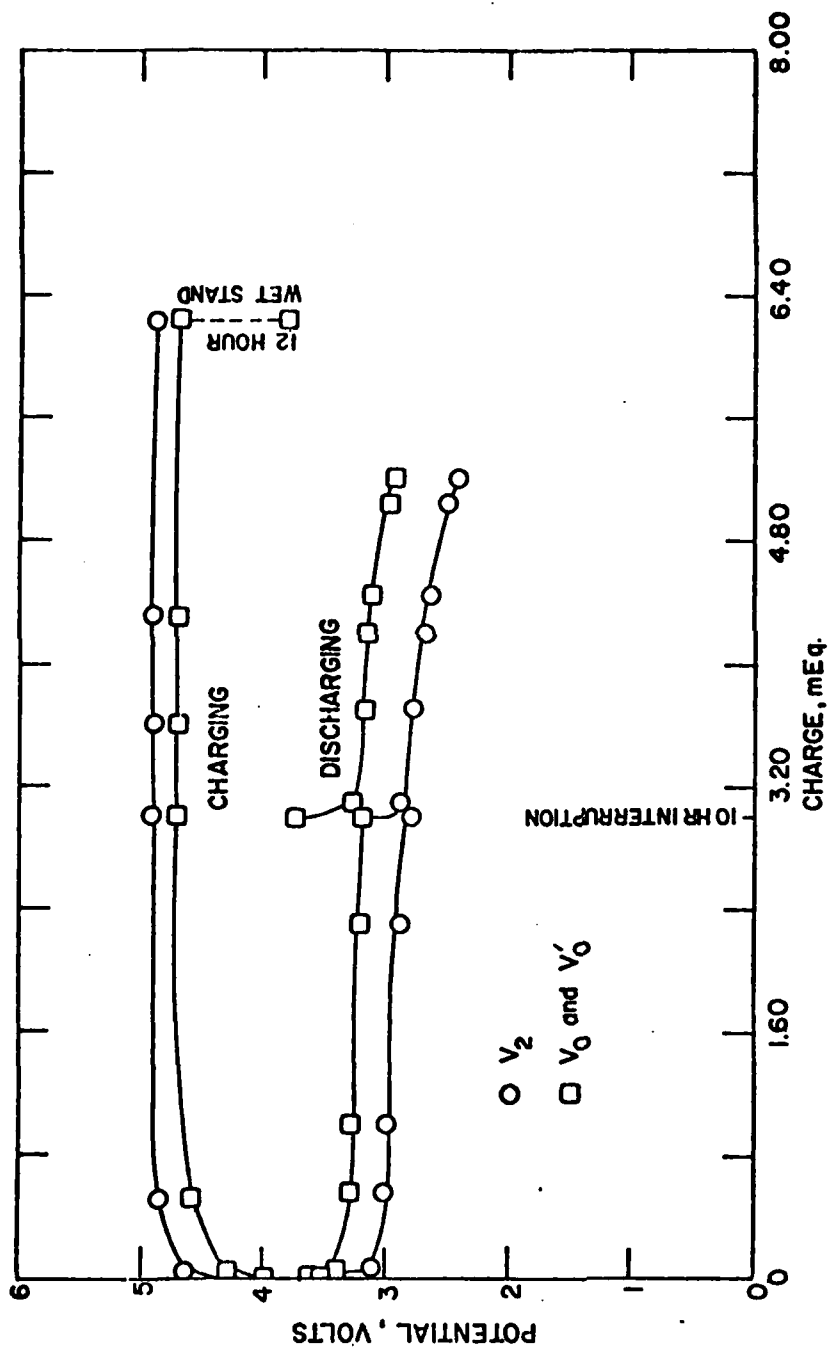


Figure 9. Galvanostatic charge-discharge curves for the cell Li/LiClO_4 , DMSO (1.0M)/Graphite Glue on Carbon cloth. Cycle No. 3. $I = 6.3 \text{ mA}$. $Q_{in} = 6.23 \text{ mEq}$. Coulombic Eff. = 83.4% above $V_f = 2.50\text{V}$. Discharge begun after 12 hours of wet stand on charge. Positive electrode weight = .7245g. Graphite = 0.2318g. Carbon cloth = 0.3735g. Initial thickness of carbon disc = 0.1 cm. Top surface area = 3.14 cm^2 . Resistance = 1.0 ohm .

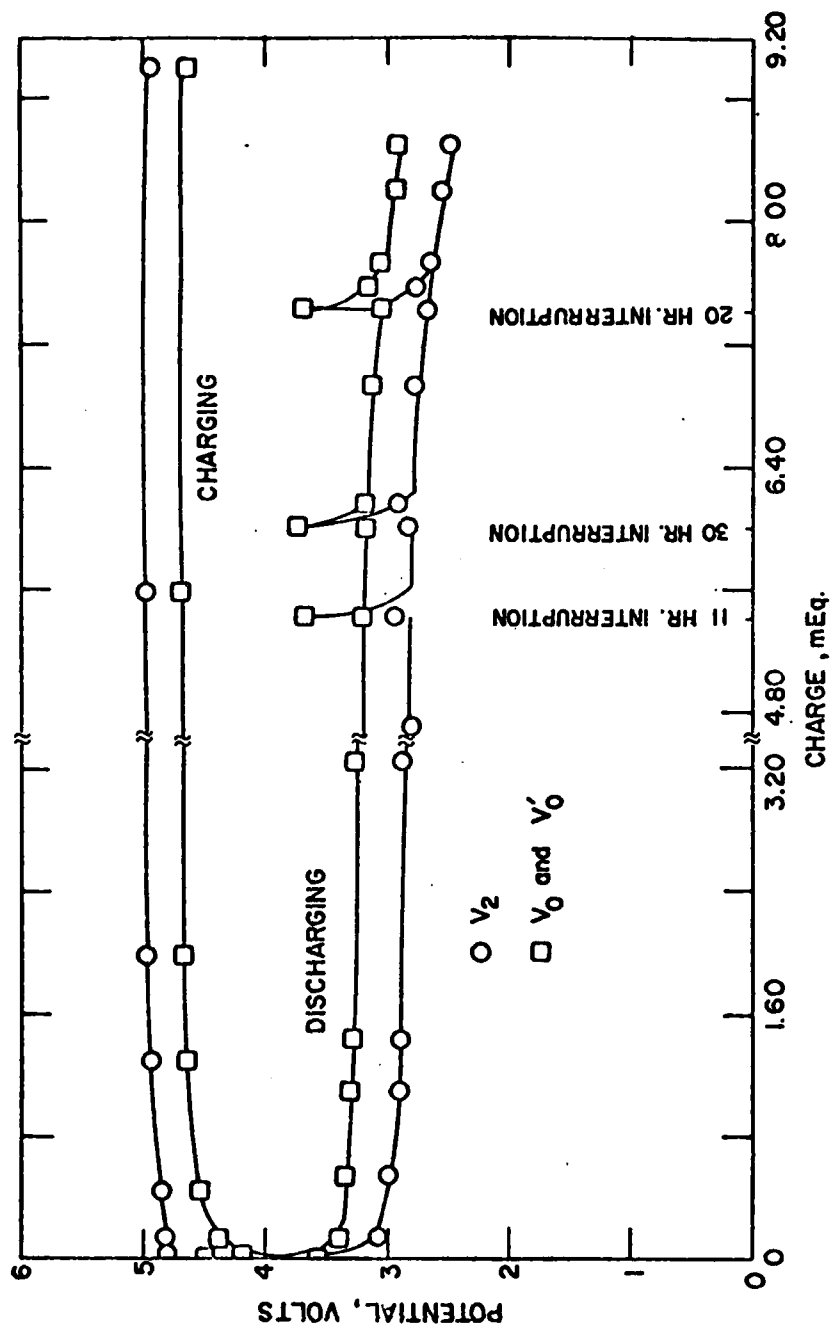


Figure 10. Galvanostatic charge-discharge curves for the cell Li/LiClO_4 DMSO (1.0M)/Graphite + Graphite glue on Carbon cloth. Cycle No. 4. $I = 6.3 \text{ mA}$. $Q_{in} = 8.92 \text{ mEq}$. Coulombic Eff. = 95.3% above $V_f = 2.50\text{V}$. Discharge begun after 0 hours of wet stand on charge. Positive electrode weight = .7245g. Graphite = 0.2318g. Carbon cloth = 0.3735g. Initial thickness of carbon disc = 0.1 cm. Top surface area = 3.14 cm^2 . Resistance = 1.0 ohm .

the first and fourth cycles, whereas on the other two cycles 10 and 12 hours of wet standing on charge was allowed. On the first cycle, two discharge plateaus were observed, one with $V_2 > 4.00$ V and the other with V_2 between 3.00 and 2.80 V. Typically, the higher plateau was not observed after the first one or two cycles depending on how deep the cycles were. The higher plateau was not observed on cycle 4. If the cell was allowed to stand on charge, the 4.00 V plateau was not observed at all, as on cycles 2 and 3.

Discharge was continued on all four cycles to a cut off voltage, $V_f = 2.50$ V. The coulombic efficiency on the first cycle exceeded 100%. The excess charge recovered was perhaps due to simultaneous discharge of impurities absorbed on the materials used in the fabrication of the positive electrode. Predictably, coulombic efficiency did not exceed 100% on the later cycles as the impurities were completely discharged during the first cycle. V_0 followed V_2 closely on the discharge runs, but the overpotential at the positive electrode, represented by $V_0 - V_2$, was greater than the overpotential, $V_2 - V_0$, during charging. In the beginning of the first cycle, $V_2 - V_0$ during the charging run was larger than $V_0 - V_2$ on discharging, but decreased as the run progressed. When V_2 had attained its peak value on charging, $V_2 - V_0$ was indeed smaller than $V_0 - V_2$ on discharging.

Ohmic losses due to the internal resistance of the cell were typically 0.75 V/mA at the beginning of the experiment and increased to 1.15 V/mA as the cell was cycled. Ohmic losses are calculated by taking the difference between the cell potential V_1 and the potential V_2 , and dividing it by the operating current. The ohmic losses are equivalent to

an internal resistance of 750 to 1150 ohms. The internal resistance is certainly high. But that is an artifact of the H-cell design where the electrodes are isolated in the two compartments. The cell potential V_1 ranged from 7.30 V to 12.10 V on charging and between -0.03 V to -4.20 V depending on the operating current and the stage of cycling.

The discharge run was interrupted on the third and fourth cycles for several hours. On every occasion, the open circuit potential of the cell was found to have drifted up to $V'_0 = 3.75$ V. On the other hand, when the cell was allowed to stand on charge after the charging run (on cycles 2 and 3), the open circuit potential was found to have drifted down to $V'_0 = 3.75$ V. Thus, after long periods of wet stand, the open circuit potential of the cell was found to attain 3.75 V reversibly. The discharge characteristics were not affected by these long interruptions as is evident from the continuous nature of discharge curves in Figures 9 and 10. The absence of discontinuities in the discharge curves in spite of the extended periods of wet stand is indicative of shelf life capability of the battery.

The amount of charge recovered during the discharge run on the four cycles is comparable to that achieved by Hebbard (31) and much greater than Dunning et al (10). Expressed in terms of coulombs per gram of graphite, the reversible electrical storage on the four cycles is 658.3, 1500.0, 2164.8 and 3541.7. If all the carbon in the electrode that is immersed in the solution contributes to the electrical storage, the weight of the glue and the part of the carbon cloth submerged in the solution must be added to the weight of graphite to give the "total" carbon content of the electrode, which was 0.5751 g (approximately 60% of

the cloth was immersed in the solution). The reversible electrical storage capacity on the four cycles was therefore 268.8, 612.8, 883.8 and 1446.0 coulombs/g "total" carbon. Before projections of energy density are made on the basis of coulombs/g "total" carbon could be made, it was necessary to determine if the electrical storage capacity was limited by the amount of graphite or "total" carbon in the positive electrode. Nevertheless, sustained discharge for 36 hours at a current density of 2 mA/cm^2 and above $V_f = 2.00 \text{ V}$ is large compared to 1 hour at 2 mA/cm^2 and 4.0 V reported by Dunning et al. (10).

It is seen from Figures 7 through 10, and even in Figures 3 through 6, that the difference between V_2 on charging and V_2 on discharging was as much as 2.50 V. Of this potential difference up to 0.30 V was the overpotential on charging and up to 0.40 V on discharging. The remaining gap of between 1.70 to 2.00 V, the difference between V_0 on charging and V_0 on discharging, is an irreversibility that implies poor energy efficiency. Since 100% coulombic efficiency has been achieved, a charging potential of 4.90 V and an average discharging potential of 2.80 V (values of V_2) mean the energy efficiency is 57%. The stable reversible electrode potential obtained after several hours of interruptions in charging or discharging, $V'_0 = 3.75$, lies approximately midway between V_0 on charging (4.70 V) and V_0 on discharging (3.00 V). Although the reason for the 0.75 to 1.00 V irreversibility on both sides is not well understood, one possibility is that the positive half-cell reaction has a low exchange current density on the electrode surface.

Physical changes during charge discharge cycles

A primary advantage of performing experiments in an H-cell is the

ability to observe independently the changes occurring in the two half-cells. Changes observed in the positive electrode, the negative electrode, and the solution in both half-cells are considered important in explaining the performance of the cell and are described below.

The carbon disk of the positive electrode swelled on charging. By the end of the fourth cycle, the electrode which was 1 mm thick in the beginning had swollen to 5 mm. It was rigid and hard. Adherence to the carbon cloth was very good. Resistance was found to be 3 ohms. The surface of the electrode was covered by a thin layer of a whitish, slimy deposit. Underneath the white deposit, the surface of the carbon disk appeared to be rough and was colored dull grey. The swelling of the electrode was very rapid in the first two cycles. On the last two cycles, the electrode did not swell much, if at all.

During the charging run of the first cycle, the solution in the positive half-cell gradually turned dark brown. The brown substance appeared to slowly diffuse through the separating porous glass frit into the negative half-cell. During the discharging run the diffusion seemed to have been accelerated. By the end of the discharging run, the solution in the positive half-cell had turned a very pale yellow while the solution in the negative half-cell was dark brown. On later cycles, there was no change in the appearance of the solution in either half-cell. The production of the brown substance thus appeared to be limited suggesting that it might be an impurity effect. A similar impurity effect was observed in all preliminary experiments. The dark brown solution in the negative half-cell prevented clear observation of the deposit on the negative electrode. Whenever the solution was changed, the impurity

effect would recur ultimately leaving a clear solution in the positive half-cell and a dark brown solution in the other. Another result of changing the solution was a decrease in the internal resistance of the cell from about 1150 ohms to about 750 ohms. However, the internal resistance increased as the solution in the negative half-cell turned brown again. In all these experiments, LiClO_4 obtained from K & K Labs, California, was used.

The deposit on the negative electrode could be seen during the first cycle. It was dendritic in nature and appeared to be adhering very weakly to the lithium substrate. In some of the preliminary experiments, the deposits were observed to break away upon shaking the cell. During the discharging run, as the solution in the negative half-cell turned darker, the dendritic lithium deposit appeared to turn into a gelatinous floc. As a result the solution became almost opaque. The floc appeared to increase on further cycling and it was impossible even to detect changes in either the lithium deposit or the solution itself in the negative half-cell.

Gassing was not observed during cycles that were short, like cycles 1 and 2. However, towards the end of the charging run on the fourth cycle bubbling was steady. It appeared that the lithium wire of the reference electrode was reacting with the solution. Indeed, twice during the 36-hour discharging run, fresh lithium wire had to be used in place of an old one which had reacted away. Some gassing was observed during the third cycle also but it appeared to stop after the discharging run was started.

The physical changes observed during the four cycles of this ex-

periment, and described above, are typical of such cells and have been observed in all the experiments performed on the cells.

II. Effect of operating current:

One of the measures of performance of batteries is specific power density. One of the variables that determine the power density is the current at which the battery is operated. To study the effect of operating current on cell performance cells of the type Li/LiClO_4 , DMSU/Graphite positive (pyrolyzed) electrode were cycled at different currents and the corresponding charging and discharging potentials (V_2) and the coulombic efficiency were observed as indicators of performance.

A trial experiment was performed using a recycled electrode. The electrode was cycled six times in the preliminary experiment described earlier (typical cycling characteristics shown in Figure 3) and thereafter dried by exposure to the atmosphere in the dry box for three days. Then it was used in this experiment in a cell (cell 4) containing fresh solution. The cell was cycled successively at 6.3, 10.0, 16.0, 20.0 and finally 6.3 mA. The main experiment was performed using a fresh electrode and an electrolytic solution containing ultra-pure LiClO_4 . The cell was cycled successively at 3.2, 6.3, 10.0, 16.0, 30.0 and 6.3 mA. Upon cycling this cell (cell 5), the positive electrode swelled from an initial thickness of 0.10 cm to 0.60 cm, and the solution in both the half-cells turned very pale yellow. In the trial experiment, the recycled positive electrode swelled from an initial 0.40 cm to 0.50 cm. At the end of the cycling, the solution in the positive half-cell became pale yellow after turning dark brown earlier and the solution in the negative half-cell was dark brown and opaque.

Differences in these two experiments were not restricted to observed physical changes alone. In the trial experiment, the charging and discharging runs were limited to a fixed duration, three hours, and a different amount of charge in proportion to the operating current, was stored in each cycle. In the main experiment, the charging runs were confined to a fixed amount of charge, about 3.6 mEq, and the duration of the cycles differed.

The effect of operating current on coulombic efficiency is shown in Figure 11 in which the coulombic efficiency is plotted against operating current density. Coulombic efficiency is based on a cut off potential of $V_f = 2.00$ V and current density on the area of the top surface of the positive electrode, 3.14 cm^2 . One hundred percent coulombic efficiency was achieved in both experiments at current densities up to 2 mA/cm^2 . Thereafter, coulombic efficiency dropped for increasing current densities. The curve appeared to level off at current densities above 6 mA/cm^2 , and a minimum coulombic efficiency in the 35 to 40% neighborhood seems achievable even at current densities higher than 10 mA/cm^2 .

Changes in V_2 during both charging and discharging, corresponding to changes in the operating currents, are shown in Figure 12. Values of V_2 for the charging run are direct experimental data since the plateaus for V_2 were flat for most of the charging run. During the discharging run however, the plateaus for V_2 were not as flat, especially at higher operating currents. So the values for V_2 that have been plotted are average values of V_2 for the discharging run. The average values were determined by taking a time-average of the raw data for V_2 . In both

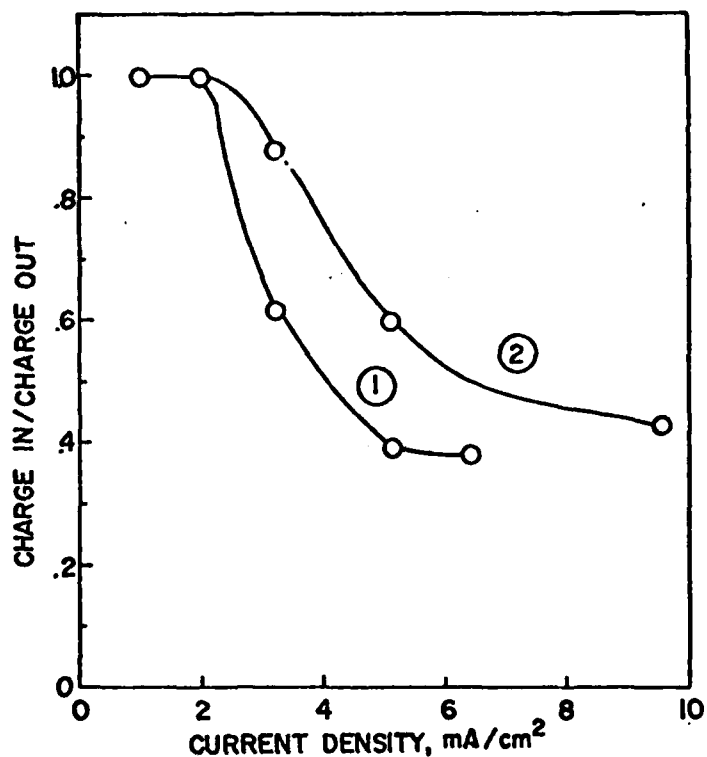


Figure 11. Effect of operating current density on coulombic efficiency (based on a cut-off potential of $V_f = 2.0V$).

Particulars of the two experiments:

		1 TRIAL EXPERIMENT	2 MAIN EXPERIMENT
Pyrolized graphite positive electrode:			
History		Recycled	Fresh
Weight of electrode	g.	0.5468	0.7048
Weight of carbon cloth	g.	0.3893	0.5032
Graphite content	g.	0.1040	0.1332
Area of top surface	sq.cm.	3.14	3.14
Swelling, from-,to	cm.	0.4 to 0.5	0.1 to 0.6
Resistance	ohms.	5.0	3.0
Electrolyte source		K & K Labs	Anderson
Brown substance observed		Yes	No
Restriction on charging runs		Duration, 3 hours	Charge, 3.6mEq.

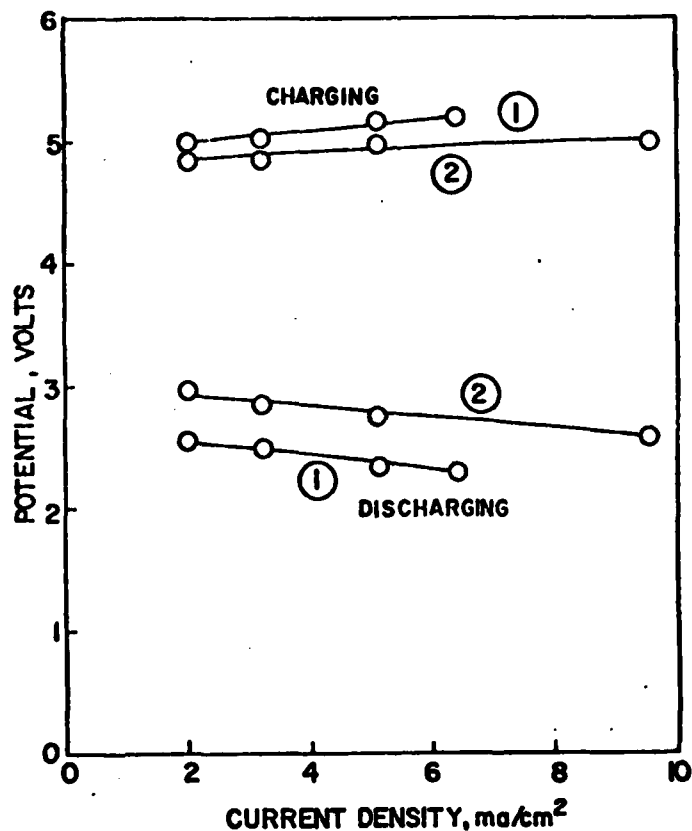


Figure 12. Effect of operating current density on the potential of the positive electrode versus the lithium wire reference electrode, V_2 , during the charging and discharging runs.

Particulars of the two experiments:

	1	2
	<u>TRIAL EXPERIMENT</u>	<u>MAIN EXPERIMENT</u>
Pyrolized graphite positive electrode:		
History	Recycled	Fresh
Weight of electrode g.	0.5468	0.7048
Weight of carbon cloth g.	0.3893	0.5032
Graphite content g.	0.1040	0.1332
Area of top surface sq.cm.	3.14	3.14
Swelling, from-,to cm.	0.4 to 0.5	0.1 to 0.6
Resistance ohms.	5.0	3.0
Electrolyte source	K & K Labs	Anderson
Brown substance observed	Yes	No
Restriction on charging runs	Duration, 3 hours	Charge, 3.6mEq.

experiments, the rate of increase in V_2 with current density on charging is slower than the rate of decrease in V_2 on discharging. In the trial experiment, V_2 increased by 0.15 V on charging and decreased by 0.20 V on discharging over the same range (2.0 to 6.4 mA/cm²) of current densities. In the main experiment, V_2 increased by 0.20 V on charging and decreased by 0.35 V during discharging over the 2.0 to 10.0 mA/cm² range of current densities. The difference between values of V_2 on charging and discharging (up to 2.80 V in the trial experiment and 2.40V in the main experiment) includes the overpotentials at the positive electrode during charging and discharging (together equal to 0.70V) and the 1.50 V to 2.00 V unexplained irreversibility mentioned earlier.

Coulombic efficiency was lower in the trial experiment than in the main experiment for all current densities greater than 2 mA/cm², and the difference between values of V_2 on charging and discharging was greater in the trial experiment than in the main one. The relatively poor performance in the trial experiment is believed to be largely due to the recycled positive electrode. The effect of the other two differences pointed out earlier, the brown substance impurity effect and the extent of charging runs, on the two observed indicators of cell performance is considered to be insignificant. The recycled electrode had a higher resistance (5.00 ohms compared to 1 ohm) than the fresh electrode and the consequent higher overpotential could have led to the observed poor performance.

It must be pointed out that in both experiments, one cycle was carried out at 6.3 mA after operating at higher currents, and the coulombic efficiency was again 100%. Charging and discharging potentials

(V₂) were the same as those obtained in the earlier cycle at 6.3 mA.

The solution in the cell did not turn brown in the main experiment. In all earlier experiments the solution in the negative half-cell was dark brown and opaque. Therefore, the changes occurring on the negative electrode and in the negative half-cell were clearly observed for the first time. The dendritic deposits of lithium on the negative electrode were found to turn into a white floc upon wet standing on charge and during the discharging run. It seems reasonably certain that the brown floc observed in earlier experiments was actually the same white floc which appeared brown because the solution was colored. The transformation of lithium deposits to white floc agrees with the observation of Selim and Bro (28). Since lithium itself was used as the substrate for lithium deposition at the negative electrode, the cell capacity was not limited by lithium. Therefore, the spontaneous conversion of lithium deposits did not result in the loss of capacity. However, in view of this observation, questions of solvent compatibility arise necessitating investigation of the specificity of the observed performance to the solvent, DMSU.

The absence of the undesirable impurity that led to the formation of the brown substance in the electrolytic solution is due to the use of ultrapure LiClO₄ acquired from Anderson Physical Labs, Illinois, in place of pure LiClO₄ purchased from K and K Labs, California, which appears to have been the source of impurity.

Specificity of the Observed Performance of the Lithium Graphite
Battery System to its Components

I. Electrolyte and solvent:

Performance of the Li/Electrolyte, Solvent/Pyrolyzed Graphite-positive battery system using LiClO_4 -DMSU electrolytic solution (cell 3) has been described above. The specificity of that performance to either LiClO_4 or DMSU was tested in three experiments in which either or both of these components of the electrolytic solution were replaced.

In one of the experiments, propylene carbonate (PC) was substituted for DMSU as solvent. LiClO_4 was used as electrolyte in this cell (cell 6). The concentration of the LiClO_4 -PC solution in the cell was 0.89 moles LiClO_4 /1000 ml solution and the open circuit potential when the cell was assembled was 2.00 V. Charge discharge curves for the cell are shown in Figures 13, 14, 15, 16 and 17. As the cell was cycled, the cell performance improved in that, on any cycle, coulombic efficiency was higher and the plateau for V_2 during the discharging run was flatter than on the previous cycle. One exception was cycle 4 (Figure 16) on which the coulombic efficiency of 58.5% was higher than the 45.2% achieved on cycle 5 (Figure 17), above a cut-off potential of $V_f = 2.00\text{V}$. The largest charge was recovered on cycle 5 with $Q_{2V} = 2.26 \text{ mEq}$. Very little charge, 0.05 mEq on cycles 2 and 4 (Figures 14 and 16), was recovered with $V_2 = 4.00 \text{ V}$.

In another experiment, a solution of LiBF_4 in DMSU (1.03 moles LiBF_4 /1000 ml solution) was used. Thus, in this cell (cell 7), the electrolyte of cell 3 was replaced. The open circuit potential of the cell was 3.00 V when filled. Figures 18, 19, 20, 21 and 22 show the

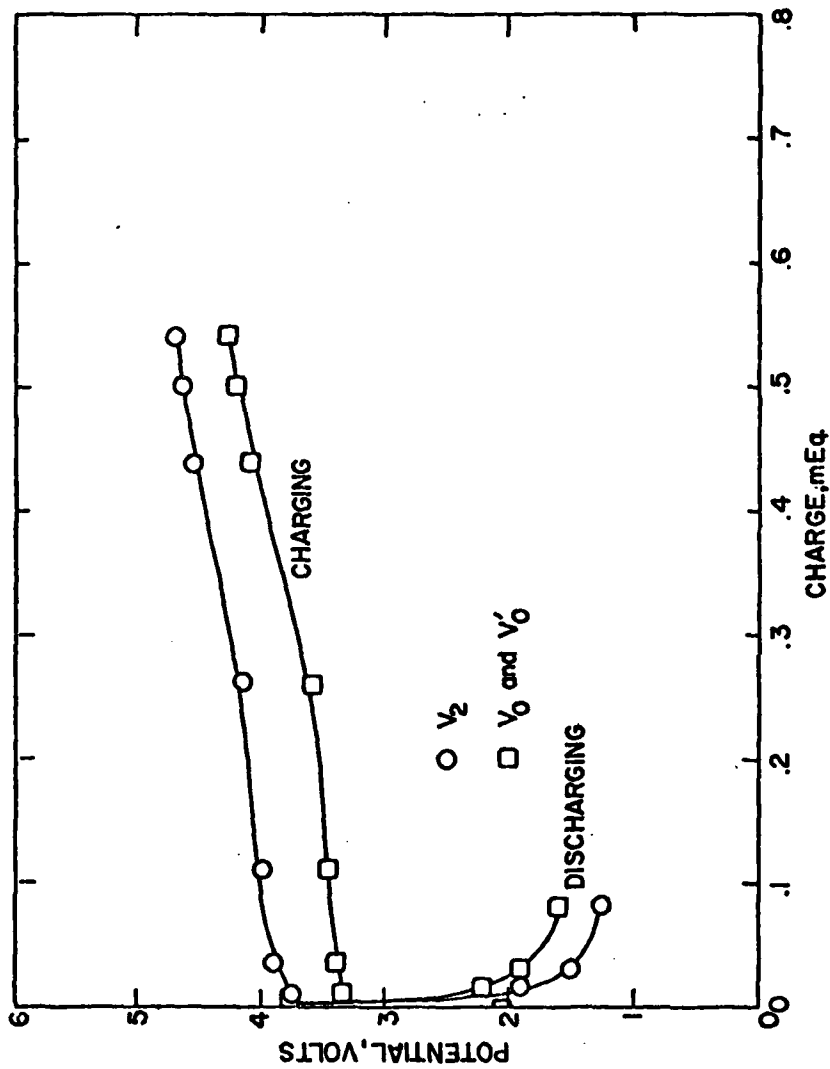


Figure 13. Galvanostatic charge-discharge curves for the cell Li/LiClO_4 , PC (0.89M)/Graphite + Graphite glue on Carbon cloth. Cycle No. 1. $I = 3.2 \text{ mA}$. $Q_{\text{in}} = 0.54 \text{ mEq}$. Coulombic Eff. = 1.85% above $V_f = 2.0\text{V}$. Positive Electrode weight = 0.6260g. Graphite = 0.1980g. Carbon cloth = 0.3262g. Initial thickness of carbon disc = 0.10 cm. Top surface area = 3.14 cm^2 . Resistance = 1.0 ohm .

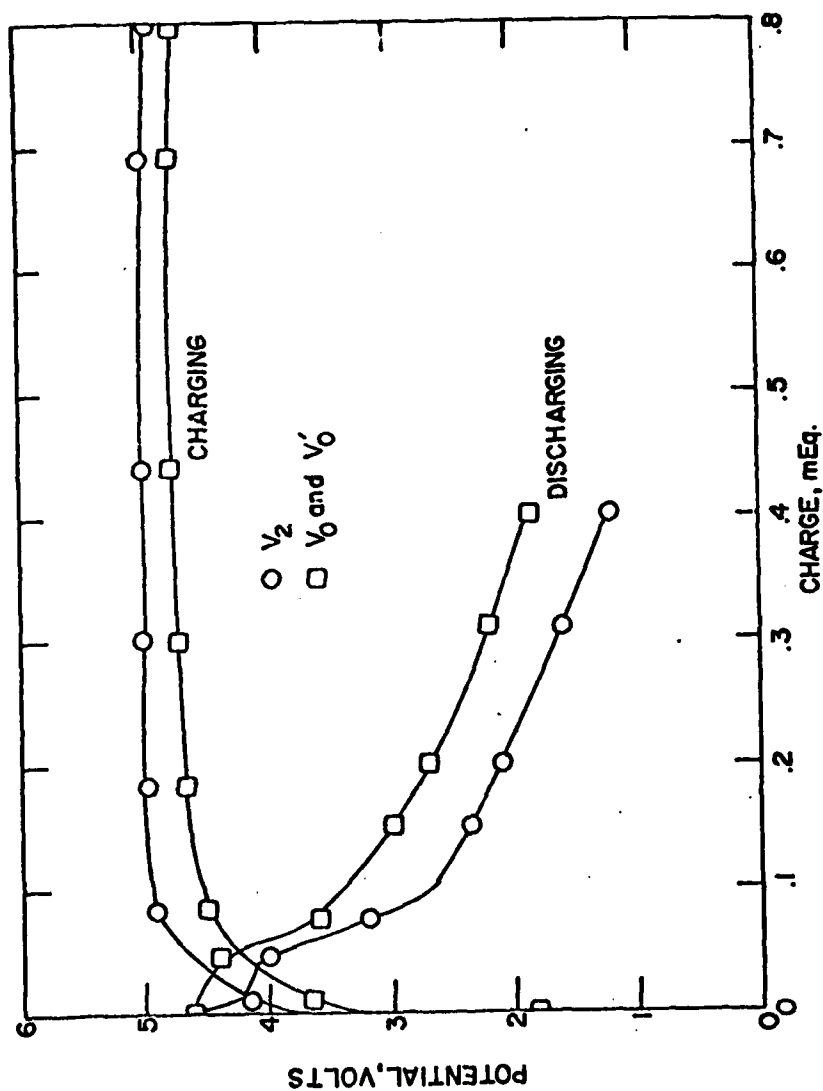


Figure 14. Galvanostatic charge-discharge curves for the cell Li/LiClO_4 , PC (0.89M)/Graphite + Graphite glue on Carbon cloth. Cycle No. 2. $I = 6.3 \text{ mA}$. $Q_{\text{th}} = 0.8 \text{ mEq}$. Coulombic Eff. = 28.75% above $V_f = 2.0\text{V}$. Positive Electrode weight = 0.6260g. Graphite = 0.1980g. Carbon cloth = 0.3262g. Initial thickness of carbon disc = 0.10 cm. Top surface area = 3.14 cm^2 . Resistance = 1.0 ohm.

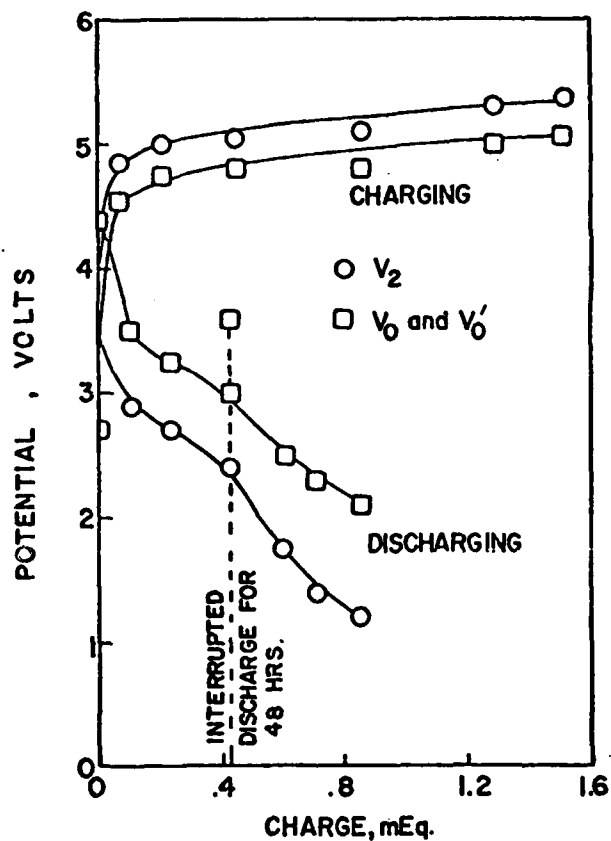


Figure 15. Galvanostatic charge-discharge curves for the cell Li/LiClO_4 , PC (0.89M)/Graphite + Graphite glue on carbon cloth. Cycle No. 3. $I = 6.3 \text{ mA}$. $Q_{in} = 1.52 \text{ mEq}$. Coulombic Eff. = 33.8% above $V_f = 2.0\text{V}$. Positive Electrode weight = 0.6260g. Graphite = 1.980g. Carbon cloth = 0.3262g. Initial thickness of carbon disc = 0.10 cm. Top surface area = 3.14 cm^2 . Resistance = 1.00 ohm.

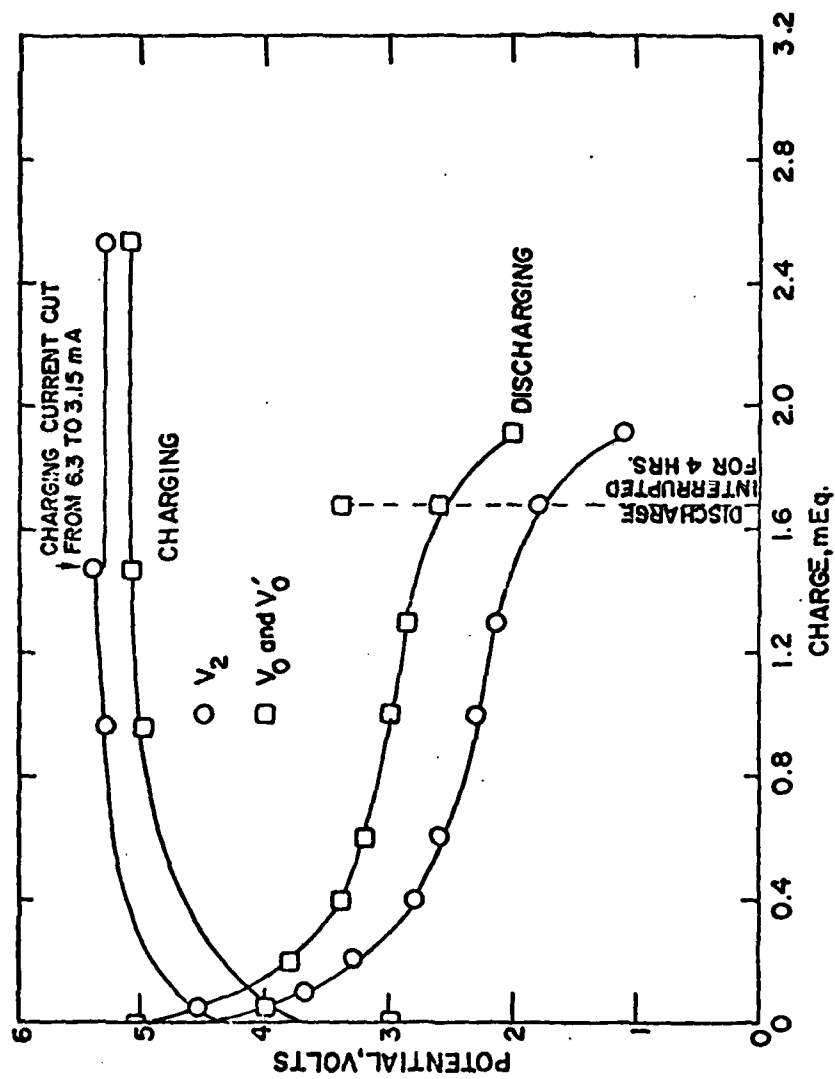


Figure 16. Galvanostatic charge-discharge curves for the cell Li/LiClO_4 , PC (0.89M)/Graphite + Graphite glue on Carbon cloth. Cycle No. 4. $I = 6.3$ mA. $Q_{in} = 2.53$ mEq. Coulombic Eff. = 58.5% above $V_f = 2.0$ V. Positive Electrode weight = 0.6260g. Graphite = 0.1980g. Carbon cloth = 0.3262g. Initial thickness of carbon disc = 0.1 cm. Top surface area = 3.14 cm^2 . Resistance = 1.00 ohm.

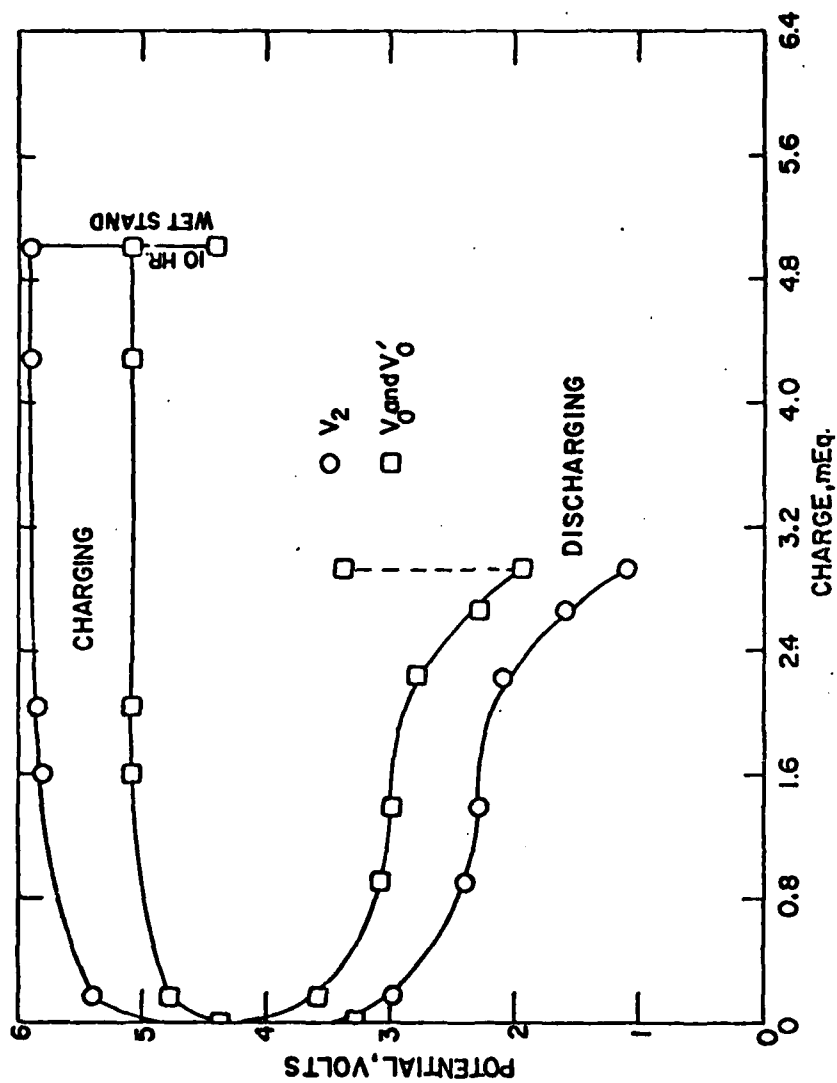


Figure 17. Galvanostatic charge-discharge curves for the cell Li/LiClO_4 , PC (0.89M)/Graphite + Graphite glue on Carbon Cloth. Cycle No. 5. $I = 6.3 \text{ mA}$. $Q_{in} = 5.0 \text{ mEq}$. Coulombic Eff. = 45.6% above $V_f = 2.0\text{V}$. Positive Electrode weight = 0.6260g. Graphite = 0.1980g. Carbon 2 cloth = 0.3262g. Initial thickness of carbon disc = 0.10 cm. Top surface area = 3.14 cm^2 . Resistance = 1.0 ohm .

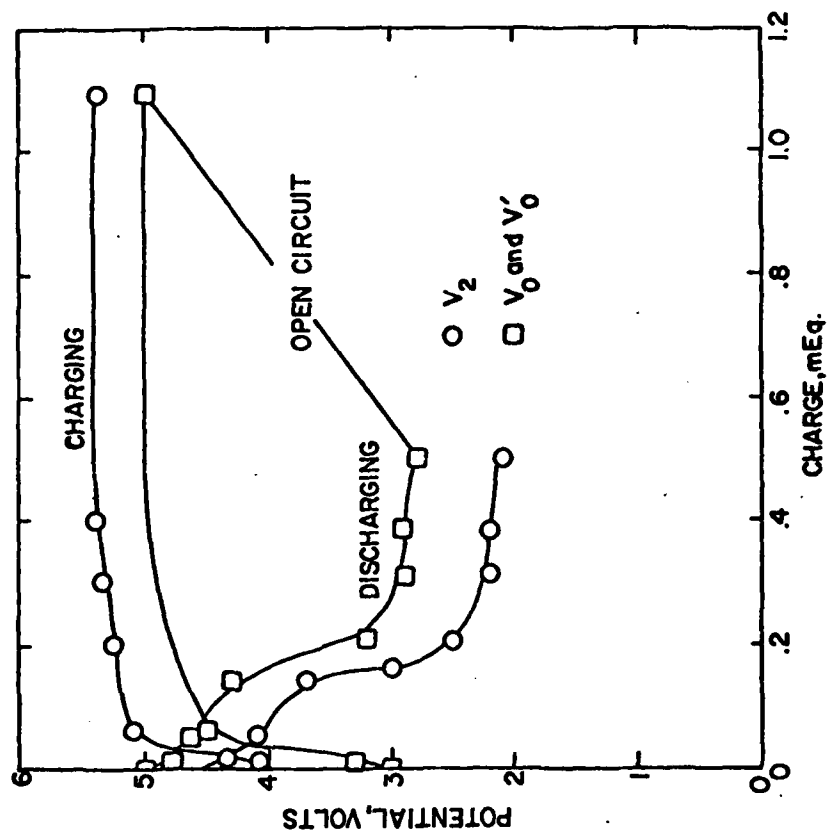


Figure 18. Galvanostatic charge-discharge curves for the cell Li/LiBF_4 , DMSU (1.03M)/Graphite + Graphite glue on Carbon cloth. Cycle No. 1. $I = 3.2 \text{ mA}$. $Q_{1\eta} = 1.09 \text{ mEq}$. Coulombic Eff. = 45.9% above $V_f = 2.10\text{V}$. Positive Electrode weight = 0.2218g. Graphite = 0.0448g. Carbon cloth = 0.1540g. Initial thickness of carbon disc = 0.04 cm. Top surface area = 3.14 cm^2 . Resistance = 3.0 ohms.

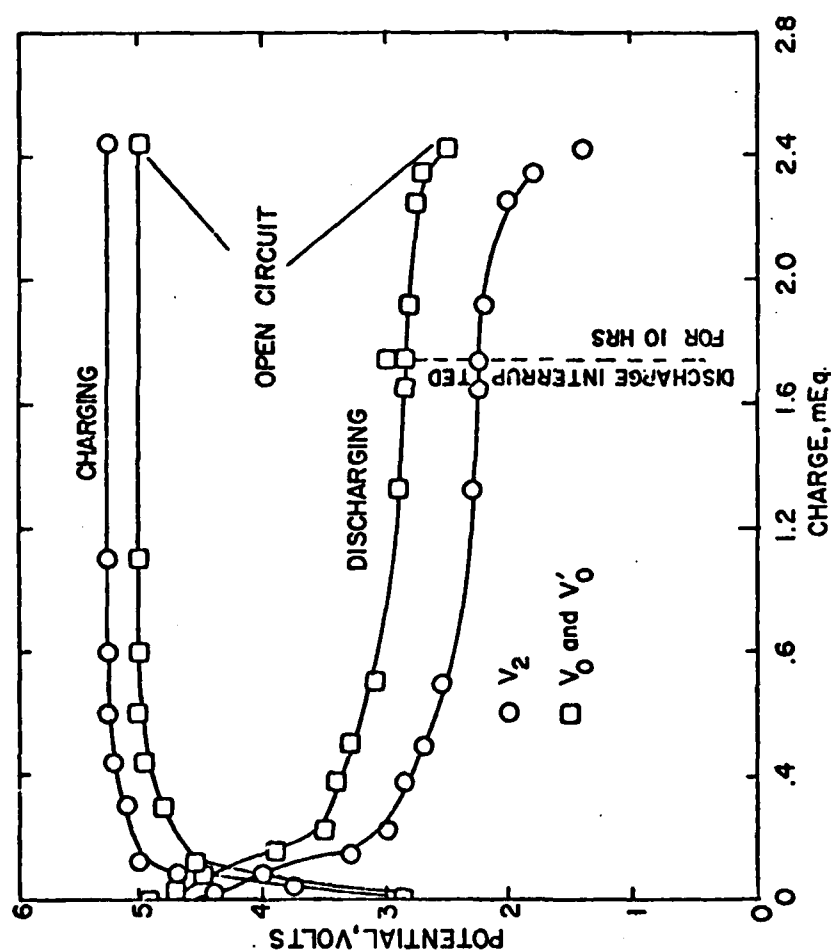


Figure 19. Galvanostatic charge-discharge curves for the cell $\text{Li/LiBF}_4\text{ (1.03M)/Graphite + Graphite glue on Carbon cloth}$. Cycle No. 2. $I = 3.2 \text{ mA}$. $Q_{\text{dis}} = 2.44 \text{ mEq}$. Coulombic Eff. = 92.3% above $V_f = 2.0\text{V}$. Positive Electrode weight = 0.2218g. Graphite 0.0448g. Carbon cloth = 0.1540g. Initial thickness of carbon disc = 0.04 cm. Top surface area = 3.14 cm^2 . Resistance = 3.0 ohms.

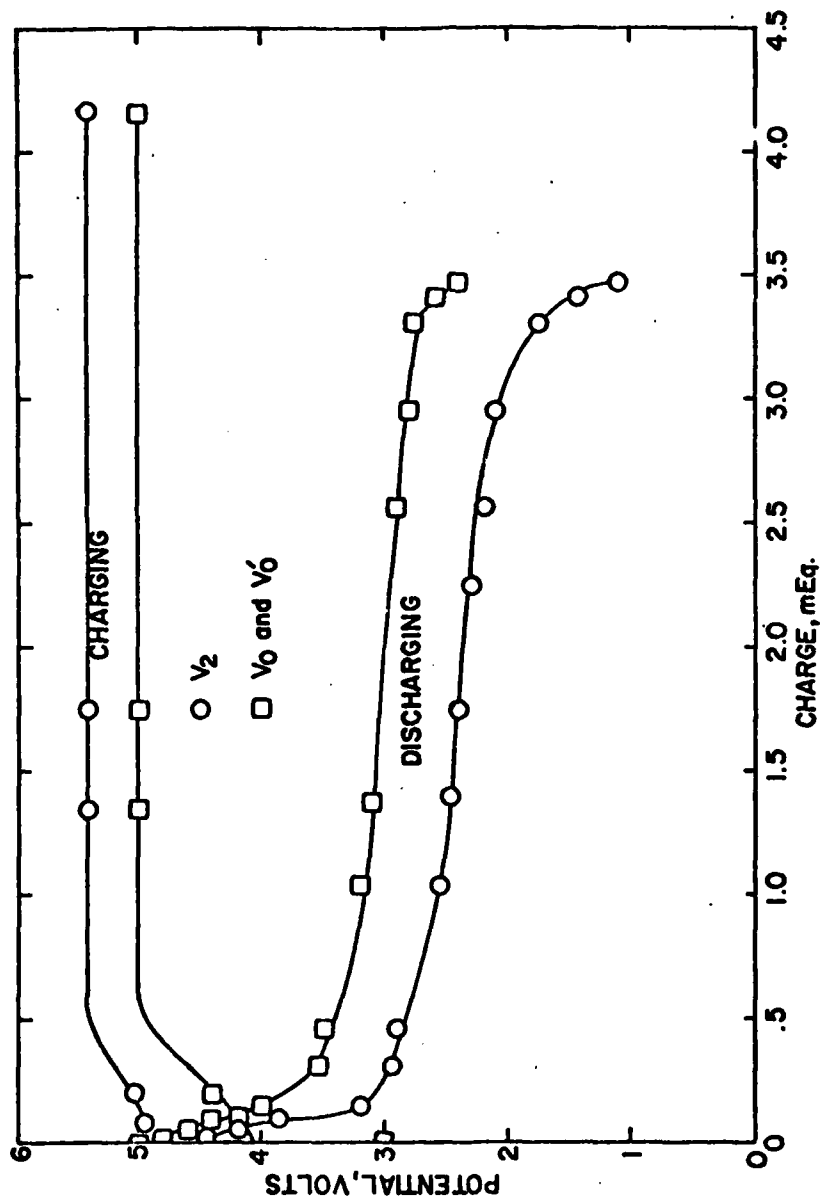


Figure 20. Galvanostatic charge-discharge curves for the cell Li/LiBF_4 , DMSU (1.03M)/Graphite + Graphite glue on Carbon cloth. Cycle No. 3. $I = 6.3 \text{ mA}$. $Q_{\text{in}} = 4.16 \text{ mEq}$. Coulombic Eff. = 72.3% above $V_f = 2.0\text{V}$. Positive Electrode weight = 0.2218g. Graphite = 0.0448g. Carbon cloth = 0.1540g. Initial thickness of carbon disc = 0.04 cm. Top surface area = 3.14 cm^2 . Resistance = 3.0 ohms.

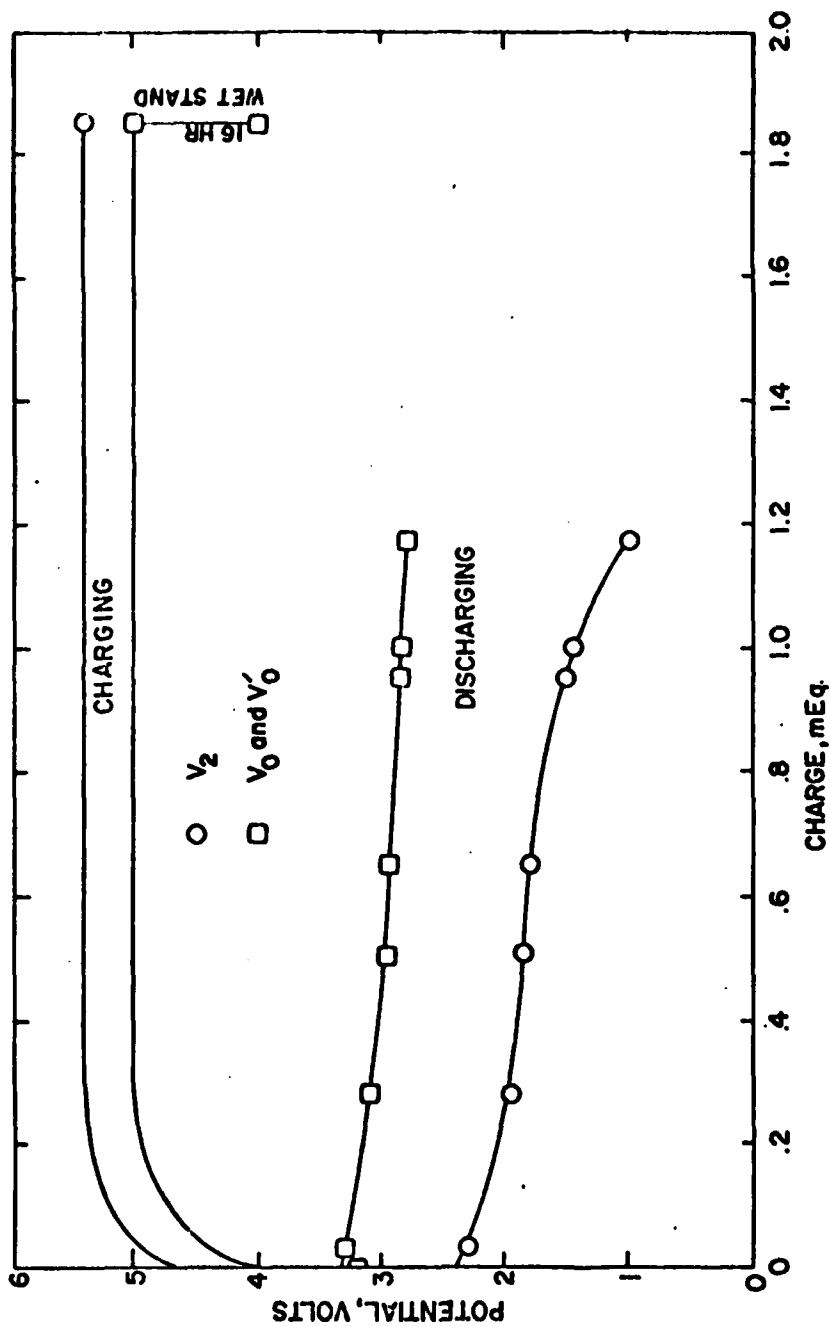


Figure 21. Galvanostatic charge-discharge curves for the cell Li/LiBF_4 , DMSU (1.03M)/Graphite + Graphite glue on Carbon cloth. Cycle No. 4. $I = 6.3 \text{ mA}$. $Q_{\text{in}} = 1.85 \text{ mEq}$. Coulombic Eff. = 14.5% above $V_f = 2.0\text{V}$. Positive Electrode weight = 0.2218g. Graphite = 0.0448g. Carbon cloth = 0.1540g. Initial thickness of carbon disc = 0.04 cm. Top surface area = 3.14 cm^2 . Resistance = 3.0 ohms.

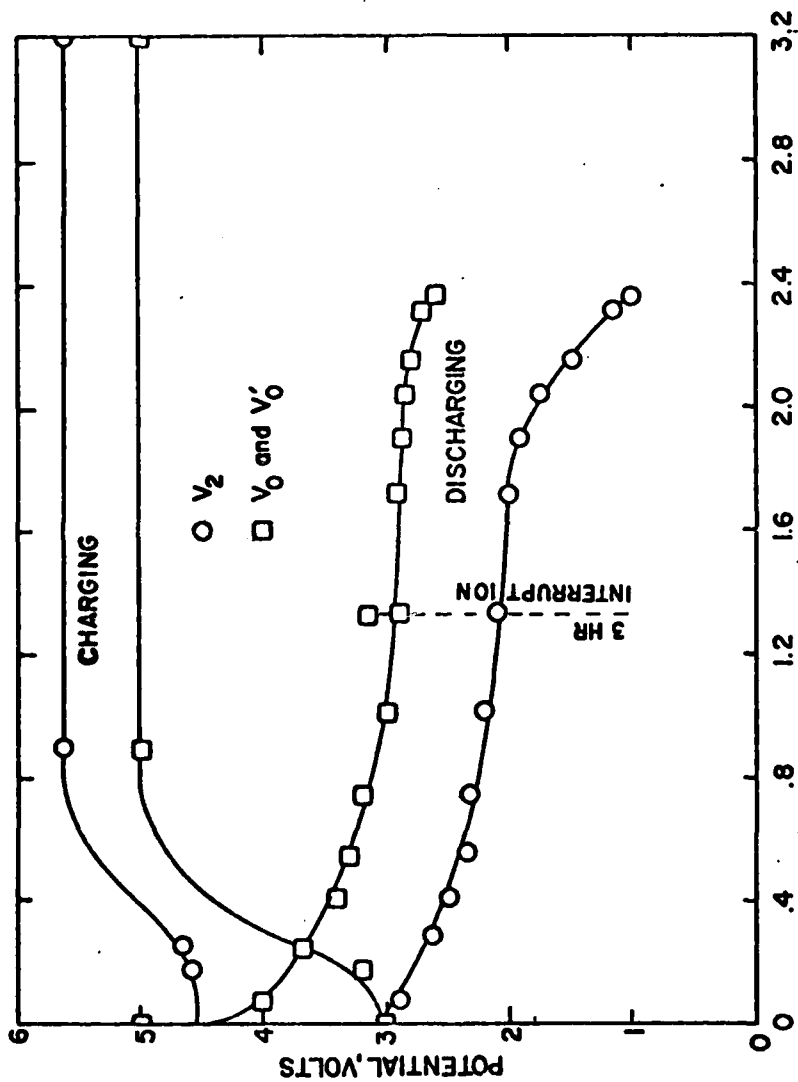


Figure 22. Galvanostatic charge-discharge curves for the cell Li/LiBF₄/DMSU (1.03M)/Graphite + Graphite glue on Carbon cloth. Cycle No. 5. $I = 6.3$ mA. $Q_{10} = 3.20$ mEq. Coulombic Eff. = 59.8% above $V_f = 2.0$ V. Positive Electrode weight = 0.2218g. Graphite = 0.0448g. Carbon cloth = 0.1540g. Initial thickness of carbon disc = 0.04 cm. Top surface area = 3.14 cm². Resistance = 3.0 ohms.

charge discharge characteristics for the five cycles. During the discharging run, the plateau for V_2 was quite flat. The charge recovered with V_2 4.00 V was very small, $Q_{4V} = 0.08$ mEq (Figures 18, 19, 20). Highest coulombic efficiency, 92% above a cut off potential of $V_f = 2.00$ V, was achieved on cycle 2 (Figure 19) and the largest charge was recovered on cycle 3 (Figure 20), $Q_{2V} = 3.00$ mEq.

The third experiment was performed using a LiBF_4 -PC solution. Thus, in this cell (cell 8) both the components of the electrolytic solution used in cell 3 were simultaneously substituted. The solution contained 1.55 moles LiBF_4 /1000 ml solution. When filled, the open circuit potential of the cell was 2.90 V. The cell was cycled three times and the charge discharge curves are shown in Figures 23 and 24. The most striking feature of this experiment was the low, nonetheless flat, plateau for V_2 , 1.50 V, during the discharging run and the high plateau, 5.70 V, during the charging run. In view of the relatively low V_2 on discharging, further study of this cell was discontinued. It must be added that discharging was stopped on cycles 1 and 2 when V_2 dropped below 1.50 V fearing solvent decomposition. Hence, the poor coulombic efficiency reported is not a true representation of performance.

A comparison of some of the operating characteristics of cell 3, 6, 7 and 8 containing different electrolytic solutions is shown in Table 2. Although substantial (over 1 mEq) charge storage has been achieved in all the cells, the charge storage in cell 3 with the LiClO_4 -DMSU solution is 2 to 3 times higher. Besides, the coulombic efficiency obtained on cell 3 was much higher in spite of a high cut off potential. If $V_f = 2.50$ V was used as the cut off potential for the other cells, the

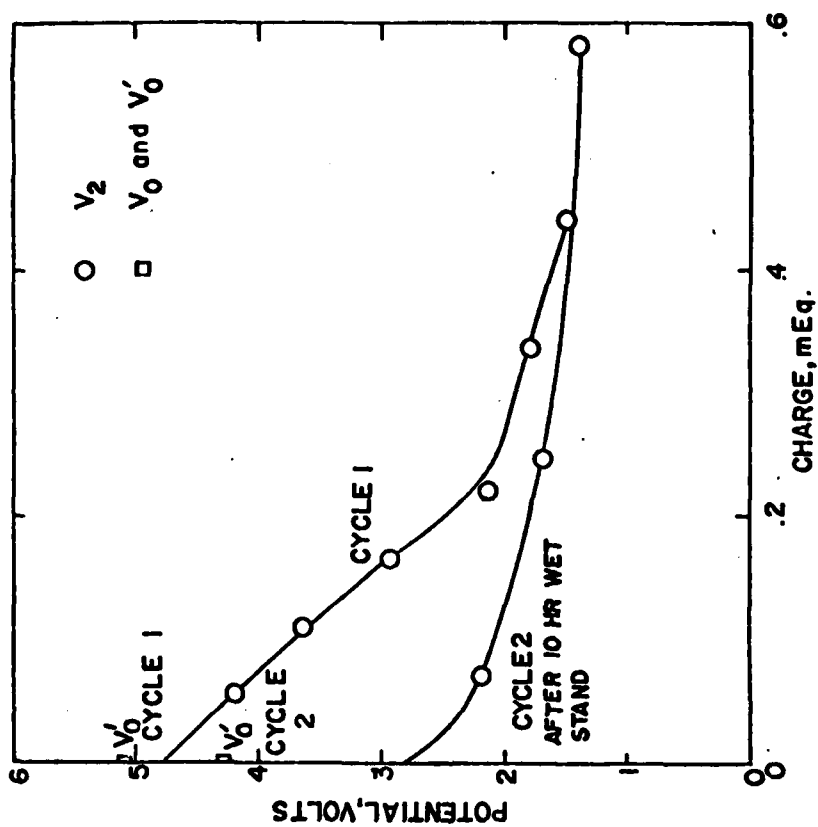


Figure 23. Galvanostatic discharge curves for cell Li/LiBF₄, PC (1.55M)/Graphite + Graphite glue on Carbon cloth. Cycle No. 1. $I = 6.3$ mA. $Q_{in} = 0.9$ mEq. Coulombic Eff. = 48.9% above $V_f = 1.50$ V. Cycle No. 2. $I = 6.3$ mA. $Q_{in} = 2.16$ mEq. Coulombic Eff. = 17.6% above $V_f = 1.50$ V. Initial thickness of carbon disc = 0.04 cm. Top surface area = 3.14 cm². Resistance = 3.0 ohms.

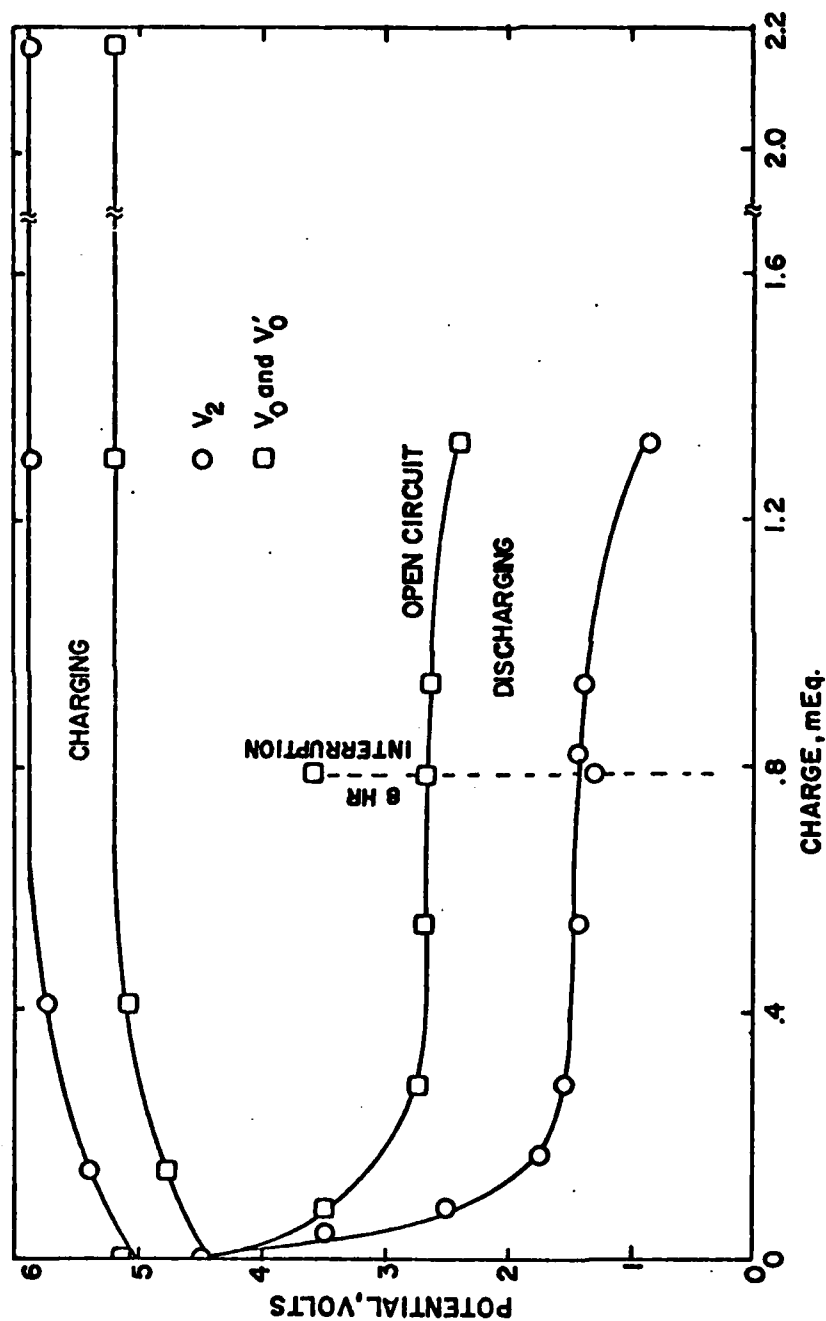


Figure 24. Galvanostatic charge-discharge curves for the cell Li/LiBF_4 , PC (1.55M)/Graphite + Graphite glue + Carbon cloth. Cycle No. 3. $I = 6.3 \text{ mA}$, $Q_{in} = 2.17 \text{ mEq}$, Coulombic Eff. = 50.0% above $V_f = 1.25\text{V}$. Positive Electrode weight = 0.1709g. Graphite = 0.0300g, Carbon cloth = 0.1200g. Initial thickness of carbon disc = 0.04 cm. Top surface area = 3.14 cm^2 . Resistance = 3.0 ohms .

TABLE 2. COMPARISON OF OPERATING CHARACTERISTIC OS LITHIUM-GRAPHITE CELL SYSTEMS CONTAINING DIFFERENT ELECTROLYTIC SOLUTIONS. ALL CELLS CONTAINED PYROLIZED GRAPHITE POSTIVE ELECTRODES.

OPERATING CHARACTERISTIC (CURRENT DENSITY 2.0 mA/cm ²)	SOLUTION IN THE CELL			
	③ LiClO ₄ -DMSU (Fig. 12)	⑥ LiClO ₄ -PC (Fig. 17)	⑦ LiBF ₄ -DMSU (Fig. 20)	⑧ LiBF ₄ -PC (Fig. 24)
Open circuit potential when filled $V_o, V.$	2.70	2.00	3.00	2.90
Steady charging potential $V_2^C, V.$	5.00	5.90	5.40	5.90
Open circuit potential, 30 secs. after interruption $V_o^C, V.$	4.70	5.10	5.00	5.20
Steady discharging potential $V_2^D, V.$	2.85	2.30	2.40	1.50
Open circuit potential, 30 sec. after interruption $V_o^D, V.$	3.20	3.00	3.00	2.70
Unexplained irreversibility $V_o^C - V_o^D, V.$	1.50	2.10	2.00	2.50
Charge recovered Q_{V_f} mEq.	8.50	2.26	3.00	1.10
with a coulombic efficiency of	95.30%	42.20%	72.30%	50.00%
above a cut-off potential $V_f, V.$	2.50	2.00	2.00	1.25
Open circuit potential upon wet stand:				
after the charging run $V_o'^C, V.$	3.75 ¹	4.40	4.00 ²	4.35 ⁴
during discharging run $V_o'^D, V.$	3.70	3.50	3.20 ³	3.60
	¹ Fig.10,11		² Fig.19 ³ Fig.21	⁴ Fig.23

coulombic efficiencies would be even lower. The potential V_2 during the discharging run for cell 3 was the highest among all four cells implying that cell 3 has the highest theoretical energy density. Cell 3 had the smallest energy losses represented by $V_2^C - V_2^D$ (from Table 2) and the smallest unexplained irreversibility, $V_0^C - V_0^D$. In addition it must be noted that, upon wet standing, only cell 3 attains a reversible open circuit potential of about 3.75 V (V_0'). Wet standing during discharging had no noticeable effect on the performance of any of the cells in that the discharge curves showed no discontinuities. However, after 16 hours wet standing on charge, coulombic efficiency above $V_2 = 2.00$ V was only 14.6% for cell 7 and the average V_2 during the discharging run was 1.80 V on cycle 4 (Figure 21) compared to 2.40 V on some other runs. It might appear that coulombic efficiency was low for cell 8 as well, after wet standing (Figure 23). But as mentioned earlier, that is an artificial observation, and should not be considered as a true representation of performance.

In the experiment with cell 3, the formation of a brown substance had interfered with clear observation of the changes occurring in the cell. In cell 6, the brown substance did appear in the positive half-cell but did not disperse into the negative half-cell, unlike in cell 3, perhaps due to the difference in solvation and electrophoretic effects in PC. A similar behavior was observed in cell 8. The occurrence of the brown substance in cell 8 was surprising because the electrolyte in that cell was LiBF_4 and not the LiClO_4 which had earlier appeared to be the source of the impurity leading to the formation of the brown substance. Accidental contamination of the solution is believed to

have led to the brown substance in cell 8. In cell 7, the solution remained pale yellow and did not turn brown.

The absence of the brown substance in the negative half-cell facilitated the observation of the lithium deposits during cycling. In all cells, the lithium deposit was found to be changing into white floc during wet stand and during discharging. Lithium deposits in cells containing PC as solvent (cells 6 and 8) were black and not shiny as in the cells (3 and 7) containing DMSU as solvent. But, in all cases the deposits were equally dendritic and poorly adhering to the substrate. Since there was no suspension in the positive half-cells, the positive electrodes were observed to swell upon cycling, in spite of the brown color of the solutions.

II. Carbon or graphite in the pyrolyzed graphite positive electrode:

Electrical storage capacity of the Lithium-Graphite battery system has been reported earlier in terms of coulombs/g graphite (10,31). Projections of the system's energy density have been made based on that measure of storage capacity. In this study the positive electrodes contained pyrolyzed graphite glue and carbon cloth in addition to natural graphite. Electrical storage capacities of up to 3541.7 coulombs/g graphite or up to 1446.0 coulombs/g "total" carbon have been demonstrated. However, it has not yet been established that the pyrolyzed graphite glue and the carbon cloth are involved in the reactions at the positive electrode. Three experiments were performed to establish the need for graphite in the positive electrode and then the role of the pyrolyzed glue and carbon cloth in the electrical storage.

In the first experiment, bare platinum was used as the positive

electrode. The open circuit potential of this cell (cell 9) when assembled was $V_0 = 2.70$ V. During charging V_2 was 5.60 V and the $V_2 - V_0$ overpotential was 1.60 V at a current of 6.3 mA (2 mA/cm^2). Up to 1.1 mEq were put in during the charging runs. When the cell was discharged, V_2 dropped very rapidly and, at best, 20% of the charge put in was recovered above zero Volts. The maximum coulombic efficiency achieved was a poor 4.74% above $V_f = 2.50$ V. At 6.3 mA (2.0 mA/cm^2) the $V_0 - V_2$ overpotential was 3.73 V. When the cell was allowed to stand on charge for 10 hours, the open circuit potential was $V_0' = 3.70$ V. No charge was recovered upon discharging the cell. Thus it was clear that platinum alone is not sufficient to achieve any reasonable charge storage in the battery.

A positive electrode consisting of pyrolyzed graphite glue on carbon cloth was used in the cell (cell 10) in another experiment. Typical charge discharge curves for cell 10 (cycle 2) are shown in Figure 25. It is seen that 4.2 mEq were recovered with 84% coulombic efficiency above $V_f = 2.50$ V beyond which the potential dropped rapidly. At a current of 6.3 mA, the discharging run lasted almost 18 hours. Other operating characteristics are reported in Table 3.

The third experiment was performed on a cell (cell 11) containing carbon cloth as positive electrode. Discharge curves for the four cycles on cell 11 are presented in Figure 26. At 6.3 mA, V_2 was 5.20 V during the charging runs in all the cycles. It is interesting that performance during the discharging run improved with cycling. Above a cut off potential of $V_f = 2.50$ V, coulombic efficiency on the four cycles was 20.3, 27.8, 22.3 and 40.6%. The reason for the lower coulombic

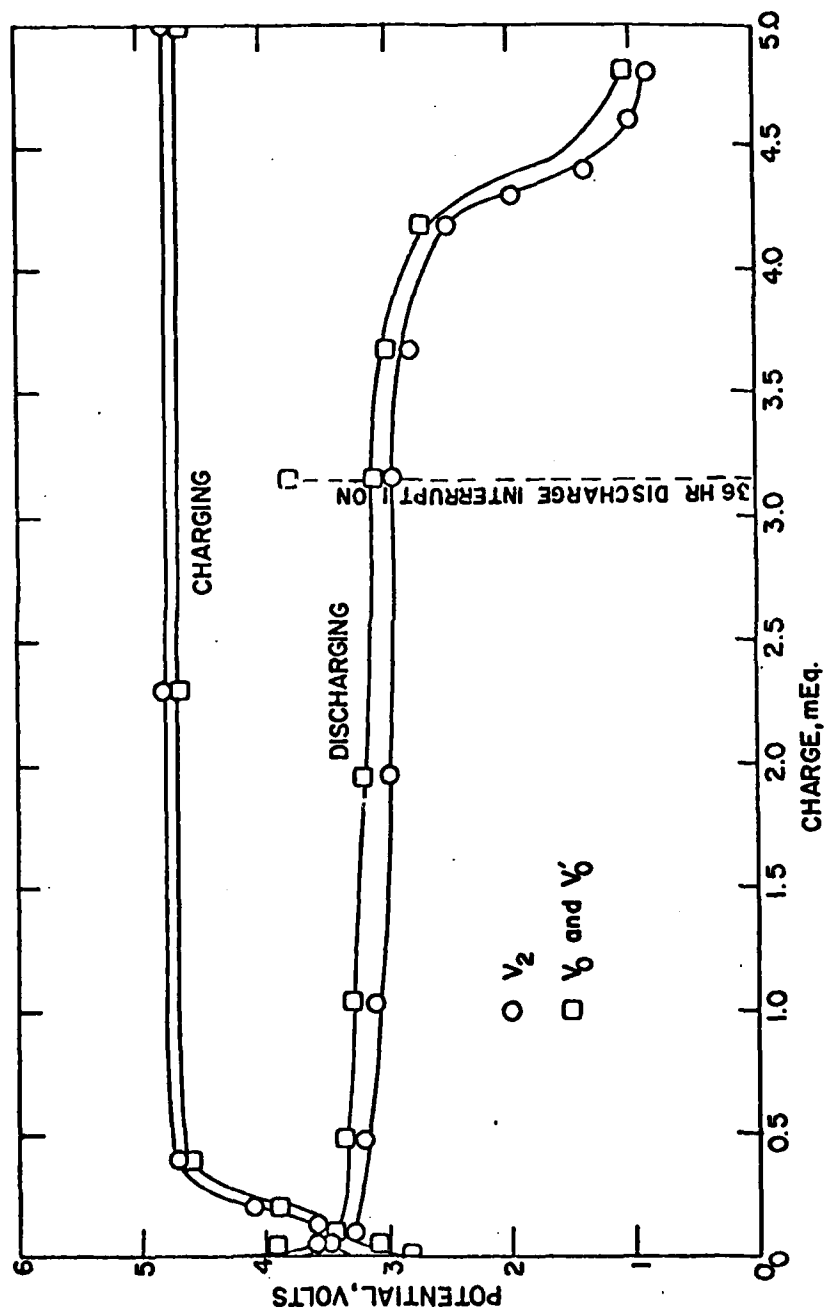


Figure 25. Typical galvanostatic charge-discharge curves for the cell $\text{Li/LiClO}_4\text{(1.53 M)/Graphite Glue on Carbon Cloth}$. Cycle No. 2. $I = 6.3 \text{ mA}$. $Q_{in} = 5.0 \text{ mEq}$. Coulombic Eff. = 64.0% above $V_f = 2.50 \text{ V}$. Positive Electrode weight = 0.7258g. Carbon cloth = 0.5053g. Initial thickness of carbon disc = 0.07cm. Top surface area = 3.14cm². Resistance = 4.0 ohms.

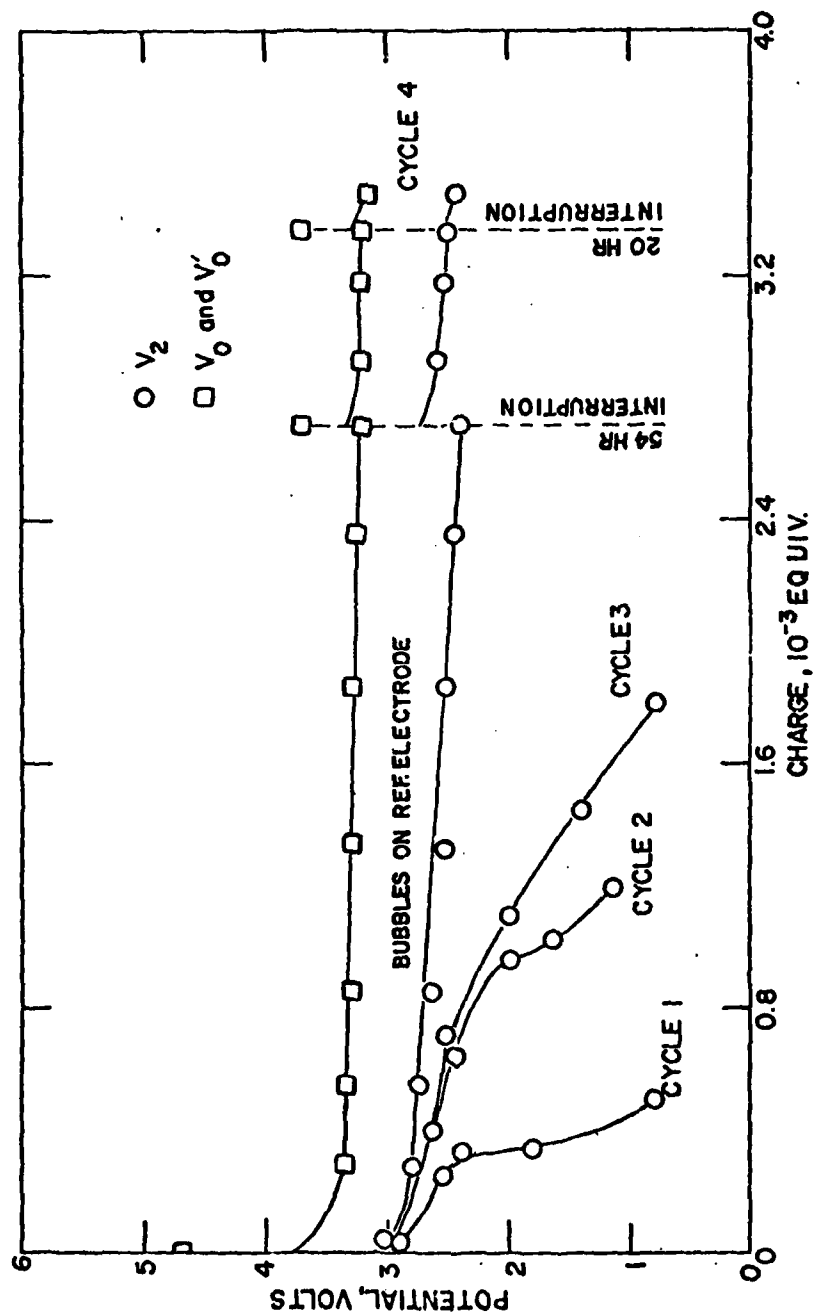


Figure 26. Galvanostatic discharge curves for the cell Li/LiClO_4 (2.13M) DMSU/carbon cloth. V_2 (charging) = 5.15V. I = 6.30 mA. Weight of carbon cloth electrode = 0.1273g. Thickness = 0.02cm. Exposed area = 3.14 cm^2 . V_0 (charging) = 4.70V.

	Cycle 1	Cycle 2	Cycle 3	Cycle 4
Charge in, 10^{-3} equiv:	1.25	2.28	3.13	8.52
Coulombic eff. above V_f = 2.50V%:	20.32	27.81	22.36	40.63

efficiency on cycle 3 than on cycle 2 is not known. On cycle 4, 3.46 mEq were recovered out of the 8.52 mEq stored when discharging was stopped because the lithium wire of the reference electrode had dissolved and the internal resistance of the cell had increased to 2.8 Kohm compared to 1.0 Kohm normally. At that time V_0 appeared to be holding steady at 3.20 V and it is possible that more charge could have been recovered and higher coulombic efficiency could have been achieved above the cut off potential, if only the solution had not become incompatible with lithium. At the end of the charging run, solution surfaces in both compartments were covered with bubbles. During the discharging run, the bubbling in the positive half-cell had become steady and appeared to be occurring at the lithium wire of the reference electrode. Bubbling continued even when discharging was interrupted overnight. In addition, the rate of evaporation of solvent in the positive half-cell appeared to have increased. One week after discharge was stopped, 30% of the solution in the negative half-cell was lost compared to all the solvent in the positive half-cell. Bubbling was also observed in cells 3 and 10 (with graphite and glue electrodes respectively) but the extent and effects (of bubbling) were not so severe.

The operating characteristics of cells 3, 9, 10 and 11 containing different positive electrodes are compared in Table 3. It is seen that significant electrical storage was achieved in cells with positive electrodes containing graphite in one form or the other (cells 3, 10 and 11). Coulombic efficiency was higher and the different operating potentials were more favorable in cells with positive electrodes containing a porous disk on the carbon cloth. Performance is somewhat

TABLE 3. COMPARISON OF OPERATING CHARACTERISTICS OF LITHIUM-GRAPHITE CELL SYSTEMS CONTAINING DIFFERENT POSITIVE ELECTRODES. ALL CELLS CONTAINED LiClO_4 - DMSU ELECTROLYTIC SOLUTION.

OPERATING CHARACTERISTIC (CURRENT DENSITY 2.0 mA/cm ²)	MATERIALS IN POSITIVE ELECTRODE			
	PT	CARBON CLOTH	GLUE ON CARB. CL.	GRAPHITE AND GLUE ON CARB. CL.
	(9)	(11)	(10)	(3)
Open circuit potential when filled. V_o , V.	2.70	2.80	2.90	2.70
Steady charging potential V_2^C V.	5.60	5.20	4.80	5.00
Open circuit potential 30 secs. after interruption V_o^C V.	4.00	4.70	4.70	4.70
Steady discharging potential V_2^D V.	None	2.55	2.95	2.85
Open circuit potential, 30 secs. after interruption V_o^D V.	None	3.20	3.15	3.20
Unexplained irreversibility $V_o^C - V_o^D$ V.	Large	1.50	1.55	1.50
Charge recovered Q_{V_f} mEq.	0.02	3.46	4.20	8.50
with a coulombic efficiency of above a cut-off potential V_f , V	4.74%	40.60%	84.00%	95.30%
Open circuit potential upon wet stand:				
after the charging run V_o^C V	3.70	--	--	--
during discharging run V_o^D V	--	3.70 (Fig.26)	3.80 (Fig.25)	3.75 (Fig.10,11)

better for cell 10 (glue) compared to cell 3 (graphite + glue) except for coulombic efficiency. However, the difference is not significant.

Discharge curves for cell 11 showed no plateau for solvent decomposition even though discharge was continued until V_2 dropped below 1.00 V. To determine the potential at which solvent decomposition takes place, a cell of the type Li/LiClO₄, DMSU/Carbon cloth, not previously charged, was discharged without being driven and with no external resistance in the circuit except for that of the coulometer and the ammeter. The cell maintained a potential of $V_2 = 1.80$ V and a current of 1 mA for over 24 hours. Since the cell was not previously charged and since no depolarizer was added, the sustained discharge is believed to be due to decomposition of the solvent. Ultrapure LiClO₄ supplied by Anderson Physical Labs was used in this experiment as well as in the experiments with cells 9, 10 and 11. In all of these experiments, the solution in both half-cells was pale yellow. The dark brown color observed in earlier experiments was not observed at all.

Analysis of the Solutions and the Positive Electrode

I. Infra-red spectral analysis:

Appearance of the brown color in early experiments in the solutions containing LiClO₄ acquired from K and K Labs indicated the possibility that the color was due to the decomposition of the solvent. In an attempt to determine if the solvent was indeed decomposed during cycling, samples of solution from both half-cells of a cell cycled several times were subjected to IR analysis along with a sample from the stock solution. It was hoped that comparison of the IR patterns of different samples would provide a clue to the identity of the brown

substance. However, IR patterns for all samples were identical to one another although the three solutions differed in appearance. The stock solution was clear, the solution from the positive half-cell was pale yellow and that from the negative half cell was dark brown. IR patterns for samples of different solutions contained all the peaks observed in the pattern for a sample of the solvent, DMSU. The pattern for the DMSU sample was similar to the standard Sadtler IR 46100. Thus, the brown substance, which was soluble in DMSU and could not be filtered out, apparently could not be detected by IR analysis.

II. X-ray powder diffraction analysis:

X-ray powder diffraction patterns were obtained for dried samples of positive electrodes from cells 1a, 3, 6 and 10 at the end of cycling. These patterns were compared with those for respective control samples of positive electrodes that were soaked in the same solution but were not used in any cell. Table 4 shows the relative intensities of peaks in the patterns for different test samples remaining unidentified after eliminating the common peaks between the test samples and their respective control samples. It is seen that peaks for the electrode from cell 6 (PC as solvent) are different from those of all the other electrodes which were cycled in cells that contained DMSU as solvent. The multiplicity of unidentified peaks is quite unexpected because all principal peaks for the known crystalline substances in the cell like graphite, LiClO_4 and LiF were among the peaks common to test and control samples. A search of the Fink index for identification of the substances that contain any combination of the peaks of Table 4 in their patterns proved fruitless.

TABLE 4. RELATIVE INTENSITIES OF UNIDENTIFIED PEAKS IN THE X-RAY POWDER DIFFRACTION PATTERNS FOR SAMPLES OF POSITIVE ELECTRODES FROM DIFFERENT CELLS. THE LISTED PEAKS DO NOT INCLUDE THOSE THAT HAVE NEITHER BEEN IDENTIFIED NOR OBSERVED IN THE PATTERNS OF RESPECTIVE CONTROL SAMPLES

ELECTRODE DATA			RELATIVE INTENSITY ¹ FOR PEAK WITH d in Å											
CELL	SOLUTION	CONSTITUENTS	7.76	4.42	3.97	3.48	3.18	2.79	2.68	2.60	2.39	2.23	1.95	1.80
1a	LiClO ₄ - DMSU	Graphite + LiF +graphite glue	20.8	100.0	9.6	7.2	33.6	4.8	10.8	10.0	--	5.2	4.4	--
3	LiClO ₄ - DMSU	Graphite + Graphite glue	36.9	100.0	10.8	9.2	38.5	6.2	12.3	15.4	--	7.7	10.8	--
6 ²	LiClO ₄ - PC	Graphite + Graphite glue	--	--	--	--	--	--	--	--	26.7	--	--	100.0
10 ³	LiClO ₄ - DMSU	Graphite glue	76.9	100.0	5.8	5.8	41.3	5.8	9.6	28.8	--	5.8	5.8	--

¹ Based on the intensity of the peak with d = 4.42 Å, except for the sample from cell 6.

² Relative intensity is based on the intensity of the peak with d = 1.80 Å.

³ Ultra-pure LiClO₄ was used.

'--' indicates no peak was observed.

TABLE 5. RELATIVE INTENSITIES, BASED ON THE PRINCIPAL PEAK FOR LiClO_4 WITH $d = 4.23\text{\AA}$, OF UNIDENTIFIED PEAKS IN THE X-RAY POWDER DIFFRACTION PATTERNS FOR SAMPLES OF DEPOSITS ON THE NEGATIVE ELECTRODE IN DIFFERENT CELLS. EFFECT OF PURITY OF LiClO_4 USED IN THE LiClO_4 - DMSO SOLUTION

CELL	PARTICULARS		RELATIVE INTENSITY FOR PEAK WITH d IN \AA									
			PURITY	SOURCE	9.21	4.38	4.04	3.51	3.30	2.98	2.40	1.64
1a			Pure	K and K Labs	-- ⁴	9.41	23.5	18.8	16.5	11.8	16.5	4.7
3			Pure	K and K Labs	32.0	37.1	41.9	59.7	24.2	32.3	35.5	12.9
5 [†]			Ultrapur	Anderson Physics Labs	7.9	7.9	5.3	7.9	13.2	--	--	5.3
10			Ultrapur	Anderson Physics Labs	6.4	6.4	5.1	15.4	15.4	7.7	20.5	5.1

⁴ Diffraction pattern obtained only for d less than 8.85\AA .

The deposit was vacuum dried at 100°C and 50\mu Hg for 8 hours.

Deposits in the negative electrode, in the form of a gelatinous floc, were also analyzed by X-ray diffraction. Powder diffraction patterns were obtained for deposits on the negative electrode in cells 1a and 3 (deposit was brown, LiClO_4 used in the cell was purchased from Anderson Physics Labs). All 12 peaks for LiClO_4 listed in the ASTM card were observed in the patterns of all three samples. Eight more peaks were observed in the patterns of the three samples which have not been identified. Table 5 lists the relative intensities of these eight peaks as observed in the four powder diffraction patterns. It must be noted that the intensities are lower in the case of cells 5 and 10 in which ultra-pure LiClO_4 was used. It is therefore possible that the eight peaks are due to impurities in LiClO_4 . But, then the same peaks (identified by their d values) should have been observed in the patterns for the positive electrode samples. Yet, there are no common peaks in Tables 4 and 5. The peaks in Table 5 that are close to those in Table 4 are ones with d values of 4.04, 3.48 and 2.39. None of the peaks in Table 5 was among the peaks that were common to the test and control samples of the positive electrodes and hence have not been listed.

III. Gas chromatographic analysis:

Chromatographic analysis of the solution in the positive half-cell was performed to determine if a new substance was added to the solution upon charging. Several different columns were tried. The best identification of a new substance was achieved using a Perkin Elmer Chrom W column coated with didecyl phthalate. Particulars of the column and the conditions under which the chromatograms were obtained are

given in Table 6.

Chromatograms of six different samples, listed in Table 7, were obtained. All the chromatograms were nearly identical. Three peaks identified by retention times were of principal interest. Two of these, occurring at retention times of 20 and 60 seconds were of interest because of the area under each of these peaks was different for each sample. The peak with retention time of 20 seconds has been identified to be that of water. The area under this peak differed for the samples because of differences in their water content.

The variations in the area under the peak with a retention time of 60 seconds is shown in Table 7. It is seen that the area increased for samples corresponding to increasing charge stored whereas the peak was not observed at all for the samples of the DMSU stock solution and the solution from the discharged cell. By the process of elimination, it appears that a new substance is indeed added to the solution upon charging the cell and is consumed during the discharging run.

The third peak of interest had a retention time of 100 seconds and covered a very large area. This peak represents DMSU.

The chromatographic analysis was not pursued beyond obtaining a qualitative identification of the new substance that is added to the solution upon charging.

Table 6

Chromatographic Analysis of Cell Solutions and Solvent -
Column Particulars and Operating Conditions

Packed Column: Length 6' Diameter 1/8"
Support material: Chrom W Mesh Size 80/100
Coating (Liquid phase): Didecyl Phthalate
Coating weight %: 15%
Recommended temperature: 25°C to 165°C
Perkin Elmer SPO 008-0668

Operating Conditions

Temperatures: Injector 140°C Column 100°C Detector 130°C
Filament Current: 150mA; Attenuation 128

Table 7

Chromatographic Analysis of Cell Solutions and Solvent -
Variations in Area under Peak with Retention Time of 60 Seconds

Sample	Description	Area
1	DMSU solvent	Not observed
2	DMSU+LiClO ₄ solution	Not observed
3	Cell solution, 1.27×10^{-3} equiv stored	0.8 units
4	Cell solution, 3.10×10^{-3} equiv stored	1.4 units
5	Cell solution, 6.20×10^{-3} equiv stored	3.0 units
6	Cell solution, after discharge	Not observed

Chapter 4

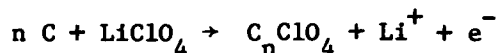
DISCUSSION

Reactions occurring at the positive electrode of the cell Li/LiClO_4 , DMSU/Graphite were the focus of this study. Nonetheless, the physical and chemical changes occurring in the cell solution and at the negative electrode were also observed carefully. Reactants in the charge-discharge processes could possibly be any or all of the materials used, namely, carbon cloth, carbonized graphite glue, natural graphite powder, the electrolyte- LiClO_4 , the solvent-DMSU, and lithium metal. Based on the results reported in the earlier chapter, the involvement of each of these constituents of the cell and their role in the cell processes can be explained.

The need for graphite in any form -- natural graphite, carbonized graphite glue, or carbon cloth -- has been demonstrated by the achievement of substantial charge storage in graphite positive electrodes and the inability of a bare platinum positive electrode to store any charge (Table 3). Thus graphite appears to be a suitable catalyst for, and possibly a participant in, the charge storage reactions at the positive electrode. When the graphite positive electrode consisted of a porous disk, coulombic efficiencies were higher while other characteristics were the same as when only carbon cloth constituted the positive electrode. This improvement in coulombic efficiency is attributed to better adsorption properties of the powders (carbonized graphite glue and natural graphite) in the porous disk than those of the carbon cloth. Between natural graphite and carbonized glue, the former appears to have better adsorption properties than the latter, as

indicated by the coulombic efficiencies in Table 3.

The porous disks of natural graphite and/or carbonized graphite glue in the pyrolyzed positive electrodes have been observed to swell as much as five times the initial thickness. This swelling may be caused by the intercalation of either the solvent or the electrolyte anion. A hypothesis for the involvement of DMSU is described later. Intercalation of perchlorate anions is characterized by the reaction

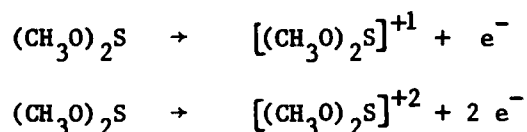


The stoichiometric coefficient may have any value greater than 1. The nonstoichiometric nature of the intercalation compound may have given rise to some or all of the unidentified peaks in the X-ray powder diffraction patterns (Table 4). The adsorption properties referred to above can be thought of as the ability to intercalate the ions in the solution.

It might be recalled (Chapter 1, Introduction) that Dunning et al (10) have suggested that intercalation of perchlorate anions was the principal charge storage reaction in the Lithium-Graphite battery. Hebbar (31) has reported a higher energy density for the same battery based on intercalation of the lighter fluoride anions as the principal charge storage reaction. In this study, substantial charge storage has been achieved using positive electrodes consisting of only carbon cloth which did not swell during cycling. It follows, therefore, that a reaction other than intercalation of anion in the graphite is a significant part of the charging process. It also appears that at least one of the products of charging, i.e., a cathode reactant, is soluble in the solution because, near the end of the prolonged charging runs, the lithium wire of the reference electrode was observed to react

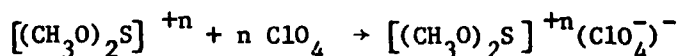
with the solution resulting in gas evolution. Furthermore, the chromatographic evidence (Table 7) of increasing concentration of a new substance in the cell solution at successive stages of the charging run, supports the soluble cathode reactant theory. Such a soluble cathodic reactant can be either or both electrolyte (LiClO_4) and solvent (DMSU). Graphite intercalation compounds are obviously not soluble. Charging reactions at the cathode are oxidation (deelectronation) processes. It is unlikely that the perchlorate anion which is already a very strong oxidizing agent is further oxidized, which leaves DMSU as the only other possible reactant.

DMSU molecules contain sulfur in the valence state 4. Since valence state 5 is possible for sulfur and 6 is common, it is reasonable to expect DMSU to be oxidized during charging. In the process, the oxidation state of the sulfur atom is raised from 4 to either 5 or 6 as characterized by the reactions



Formation of the radical cation, $[(\text{CH}_3\text{O})_2\text{S}]^{+1 \text{ or } 2}$, could be followed by, or coincident with, its adsorption on, or intercalation in, the graphite electrode so that the electroneutrality in the solution is not violated. Such intercalation of the radical cation on the electrode could cause it to swell just as considered possible due to the intercalation of perchlorate anions. The electroneutrality of the graphite is maintained by the adsorption of perchlorate ions along side the radical cations or

excess of the anions in the Gouy double layer. Perchlorate anions are free in the solution due to the simultaneous deposition of lithium at the negative electrode. Some of these may be intercalated in graphite as described earlier. It is possible that the unadsorbed radical cations and the free perchlorate anions which balance the charge on each other in the solution combine to form a neutral charge complex as per the reaction



where n is either 1 or 2. This complex could also be adsorbed on the graphite in the positive electrode.

The adsorption of the radical cation on graphite along side the anion is not unreasonable to expect. McDonnell et al (33) have found that graphite can take up electrons from potassium atoms to form compounds of the type C_8K . In a similar manner, under the influence of externally applied potential, graphite can be expected to remove electrons from both perchlorate anion and the DMSU molecule, to replenish the electrons in the fused "aromatic" nuclei of the graphite that are conducted away, during charging, to the negative electrode via the external circuit. The perchlorate radical, minus its charge, and the DMSU radical cation are then both adsorbed on the graphite surface or intercalated between the layers of aromatic nuclei. It is also possible that the perchlorate anions and the DMSU molecules do not donate their electrons before being adsorbed but instead share them with the graphite. Adsorption of the two species might be both catalytic and synergistic, continuously creating more surface area for further adsorption due to the exfoliation of graphite accompanying the adsorption. It is also possible that the

neutral charge complex is adsorbed on the graphite surface. In any case, the capacity of graphite for adsorption is eventually exhausted and further continuation of the charging run leads to the dissolution of the neutral charge complex. When the radical cations in solution contact the lithium wire of the reference electrode, it reacts to form a gaseous product. The gaseous product has not been identified yet.

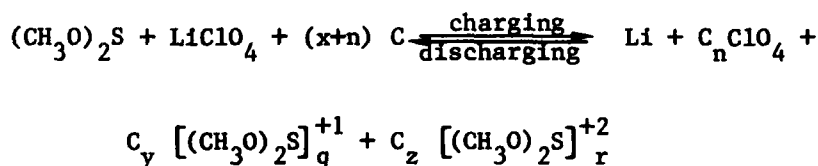
Perfect or near perfect coulombic efficiency followed by a rapid drop in potential V_2 is considered an indication of the reversibility of the charging reactions proposed above. Chromatographic evidence (Table 5) showing that the concentration of the "new" substance is negligible in the cell solution after the discharging run and that no "other new" substance is observed further strengthens the theory that the reactions during the discharging run are indeed reversals of the charging processes and not formations of more new substances by the decomposition of the solvent or the electrolyte. It must be pointed out that solvent and/or electrolyte decomposition was found to occur at $V_2 = 1.80$ V with the current at 1.0 mA whereas the discharging potential in most experiments was at $V_2 = 2.90$ V with the current at 6.3 mA. The electrode in both experiments had the same area. Less than 100% coulombic efficiency on discharging could be due to reaction of the soluble cathode reactant with the lithium wire of the reference electrode and mass transfer limitations that cause the potential to drop below the cut off potential V_f before all the cathode reactants have been utilized completely.

Reaction at the negative electrode on the other hand is simply the deposition and dissolution of lithium.



During the discharging run, the dendritic lithium deposits have been observed to change into a white floc. X-ray powder diffraction patterns of the deposit indicate that these deposits are LiClO_4 . If that is the case, it is implied that as lithium dissolves during discharging, a local supersaturation of LiClO_4 occurs near the negative electrode and the salt is precipitated. Such local supersaturation could be caused by low transference number of Li^+ cations which means that current within the cell is sustained primarily by perchlorate anions.

The overall cell reactions can then be represented as follows:



where $n > 1$, $q+r=1$ and $y+z=x > 1$.

After the adsorption capacity of the graphite has been exhausted, the radical cation is formed by deelectronation on the graphite surface and is followed by the combination with perchlorate anions in the solution to form the neutral charge complex. It might be added that the overall cell reaction involves 1 electron transfer per perchlorate anion adsorbed and either 1 or 2 electrons per solvent radical cation adsorbed.

The suggested involvement of the solvent in the charging process and the solubility of the resulting cathode reactant in the solution have significant implications about the limiting role of graphite. Traditionally, solubility of the cathode reactant has been considered highly undesirable because it led to self discharge. If that is the criterion, then the charge storage capacity of the cell is indeed

limited by the adsorption capacity of the graphite in the positive electrode for the neutral charge complex and the ions in the solution, and, may be expressed in terms of coulombs/g graphite. But, if a highly selective anion exchange membrane is available, then the lithium negative electrode can be effectively shielded from the radical cation while the current is maintained by the perchlorate ions shuttling across the membrane. In that event, the capacity for electrical storage cannot be based on a unit mass of graphite because graphite would not then be the limiting reactant. The battery system would thus be viable in spite of the solubility of the cathode reactant. At least two nonaqueous lithium secondary battery systems under development have been reported in the literature that have a soluble positive electrode. $\text{Cu}(\text{ClO}_4)_2$ and CuBr_2 are the soluble positive electrodes (also serving as electrolyte) in one study, in which Dampier et al (34) report "self discharge was suppressed by a special protective film formed on the lithium electrode." The other study has dissolved lithium polysulfides as the soluble positive electrode (35) but the mechanism of prevention of self discharge has not been indicated. Efforts to find a suitable membrane for the Lithium-Graphite battery system are now under progress (36).

The substantial charge storage achieved after substitution of materials is partly explained by the intercalation, in graphite, of the anion present in the solution. In the cell containing LiBF_4 -DMSU solution, solvent involvement, similar to that described earlier, probably contributes to the charge storage capacity. In the cells using PC as solvent, however, solvent involvement is not clear. In fact there might not be any solvent involvement. The lower charge capacities of

cells 6 and 8 might, therefore, be due to non-involvement of the solvent, with all the demonstrated charge storage capacity representing anion intercalation. Differences in other operating characteristics are believed to be due to specificity of the respective characteristics to both the electrolyte and the solvent.

Chapter 5

CONCLUSIONS

The reversible electrical storage capacity of the Li/LiClO_4 , DMSU/Graphite secondary cell has been demonstrated to be very high. It appears that fluoride ions, from the lithium fluoride additive in the positive electrode, do not participate in the reaction and are not necessary to achieve the large energy storage. The precipitation of lithium perchlorate at the negative electrode suggests that the lithium ions have low mobility in the electrolytic solution and that the current in the cell is sustained by the perchlorate ions alone.

Based on the results obtained so far, it appears that a soluble species is formed as the product of charging and it is consumed on discharging. Because of the solubility of the product of charging, the reactions in the cell are limited by the rate of mass transfer. When natural graphite is a constituent of the positive electrode, a side reaction, perhaps the intercalation of the perchlorate anion, occurs the first time the cell is charged causing the electrode matrix to swell thus creating a large surface area. The soluble product of charging is stored, probably by adsorption, on the exfoliated natural graphite.

It is proposed that one of the reactants on charging is the solvent DMSU. The charging reaction raises the oxidation state of the sulfur in DMSU to five or six from four, forming a radical cation, and that this process is reversed during discharging. Of the two plateaus ob-

served on discharging, the 4.00 V plateau is believed to represent reversal of the perchlorate ion intercalation while the one at 3.00 V is attributed to the radical cation reverting to DMSU. Irreversible decomposition of the solvent occurs at 1.80 V when the cell is not driven on discharge and the current is 0.32 mA/cm^2 .

The need for a good separator has been established to prevent self discharge due to the attack of the dissolved product of charging on the lithium electrode. Lithium deposits are dendritic, not dense, in nature and have poor adherence to the substrate.

The large difference in potential on charging and discharging is tentatively considered to be due to low exchange current densities. However, this needs to be established. The role of the solvent in the charging and discharging reactions must be studied and correlation of changes in the solvent with the amount of charge stored must be obtained as conclusive proof of the proposed reaction. Experiments with limited solvent in the cell must be performed for such correlation.

REFERENCES

1. Visser, D. R., et al. "Parametric Characterization Studies of Electrochemically Prepared Li-Al Electrodes in Li/LiCl-KCl/Li-Al Cells," Abstract No. 20, Fall Meeting of the Electrochemical Society, Dallas, 1975.
2. McPheeters, C. G., et al. "Performance and Cost Improvement in Li-Al/FeS₂ Cells through the use of Cobalt Sulfide Additives," Abstract No. 25, Fall Meeting of the Electrochemical Society, Dallas, 1975.
3. Yao, N. P., et al. "Development of Positive Electrodes for Prismatic Lithium-Aluminum/Iron Sulfide Cells," Abstract No. 26, Fall Meeting of the Electrochemical Society, Dallas, 1975.
4. Koura, N., et al. "Coated Metal Current Collectors for Iron Sulfide Electrodes in High Temperature Cells," Abstract No. 30, Fall Meeting of the Electrochemical Society, Dallas, 1975.
5. Gabano, J. P., et al. "High Energy Cells with a Lithium Electrode," Proceedings of the 23rd Annual Power Sources Conference, May 1969.
6. Brauer, K. and K. R. Moyes. "High Energy Density Batteries," U.S. Patent No. 3, 514, 337, May 26, 1970.
7. Watanabe, N. and M. Fukuda. "Primary Cell for Electric Batteries," U.S. Patent 3, 536, 532, October 27, 1970.
8. Pistoia, G. "Nonaqueous batteries with LiClO₄-Ethylene Carbonate as Electrolyte," J. Electrochem. Soc., 118(1): 153-158, January 1971.
9. Brenner, A. "Note on Organic-Electrolyte Cell with a High Voltage," J. Electrochem. Soc., 118(3): 461, March 1971.
10. Dunning, J. S., et al. "A Secondary, Nonaqueous Solvent Battery," J. Electrochem. Soc., 118(12): 1886-1890, December 1971.
11. Campanella, L. and G. Pistoia. "M₂O₃ - New Electrode Material for Nonaqueous Secondary Battery Applications," J. Electrochem. Soc., 118(12): 1905, December 1971.
12. Gabano, J. P., et al. "D-Size Lithium Cupric Sulfide Cells," J. Electrochem. Soc., 119(4): 459-461, April 1972.
13. Hunger, H. F. and G. J. Heymach. "Cathodic Discharge of Graphite Intercalation Compounds in Organic Electrolytes," J. Electrochem. Soc., 120(9): 1161-1168, September 1971.
14. Kimmerle, F. M. and G. Giasson. "Cathode Reactants in High Energy Density Aprotic Battery Systems. The Metallic Borosulfides," J. Electrochem. Soc., 120(9): 1214-1216, September 1973.

15. Auburn, J. J., et al. "Lithium Anode Cells Operating at Room Temperature in Inorganic Electrolyte Solutions," J. Electrochem. Soc., 120(12): 1613-1619, December 1973.
16. Behl, W. K., et al. "Lithium Inorganic Electrolyte Cells Utilizing Solvent Reduction," J. Electrochem. Soc., 120(12): 1619-1623, December, 1973.
17. Weininger, J. L. and F. W. Secor. "Nonaqueous Lithium-Bromine Secondary Galvanic Cell," J. Electrochem. Soc., 121(3): 315-318, March 1974.
18. Dampier, F. W. "The Cathodic Behaviour of CuS, MoO₃, and MnO₂ in Lithium Cells," J. Electrochem. Soc., 121(5): 656-660, May 1974.
19. Holleck, G.L., et al. "Transition Metal Sulfides as Cathodes for Secondary Li Batteries," Abstract No. 52, Fall Meeting of the Electrochemical Society, New York, 1974.
20. Margalit, N. "Discharge Behaviour of Li/MoO₃ Cells," J. Electrochem. Soc., 121(11): 1460-1461, November 1974.
21. Holleck, G. L. and J. R. Driscoll. "Titanium Sulfides as Cathodes for Secondary Lithium Batteries," Abstract No. 32, Fall Meeting of the Electrochemical Society, Dallas, 1975.
22. Margalit, N. "The Discharge Behaviour of Li/Ag₃ PO₄ Cells," Abstract No. 40, Fall Meeting of the Electrochemical Society, Dallas, 1975.
23. Lazzari, M., et al. "Performances of Organic Solvent Batteries Using Substoichiometric Oxides as Cathodic Materials," Abstract No. 41, Fall Meeting of the Electrochemical Society, New York, 1975.
24. Dey, A. N. "Electrochemical Studies on the Effect of H₂O in Nonaqueous Electrolytes," J. Electrochem. Soc., 114(8): 823-824, August 1967.
25. Meibuhr, S. G. "Electrode Studies in Nonaqueous Electrolytes; 1. The Lithium Electrode in LiClO₄-PC Solutions," J. Electrochem. Soc., 117(1): 56-60, January 1971.
26. Tiedemann, W. H. and D. N. Bennion. "Chemical and Electrochemical Behaviour of Lithium Electrodes in Dimethyl Sulfite, Electrolytic Solutions," J. Electrochem. Soc., 120(12): 1624-1628, December 1973.
27. Dampier, F. W. and P. E. Krouse. "The Stability of Lithium in Several Organic Electrolytes at 740C," Abstract No. 23, Fall Meeting of the Electrochemical Society, New York, 1974.
28. Selvin, R. and P. Bro. "Some Observations on Rechargeable Lithium Electrodes in a Propylene Carbonate Electrolyte," J. Electrochem. Soc., 121(11): 1457-1459, November 1974.

29. Yao, N. P., et al. "Behaviour of Dimethyl Sulfite as a Potential Nonaqueous Battery Solvent," J. Electrochem. Soc., 115(10): 999-1003, October 1968.
30. Mirza, Z. I. "Transport Properties of Lithium Perchlorate in Dimethyl Sulfite," M.S. Thesis, School of Engineering and Applied Science, University of California, Los Angeles, 1971.
31. Hebbar, R. K. "Carbon Porous Electrodes as Nonaqueous Secondary Battery Reactants," M.S. Thesis, School of Engineering and Applied Science, University of California, Los Angeles, 1974.
32. Tiedemann, W. H. "Chemical and Electrochemical Behaviour of Lithium Electrodes in Dimethyl Sulfite Solutions," Ph.D. Thesis, School of Engineering and Applied Science, University of California, Los Angeles, 1971.
33. McDonnell, F. R. M., et al. "Some Physical Properties Associated with 'Aromatic' Electrons. Part III. The Pseudo-metallic properties of Potassium-Graphite and Graphite-Bromine," J. Chem. Soc., London, 1951.
34. Dampier, F. W., et al. "Soluble Copper Positive Electrodes for Lithium Secondary Cells," Abstract No. 5, Spring Meeting of the Electrochemical Society, Washington, D. C., 1976.
35. Rauh, R. D., et al. "The Li/Dissolved S Secondary Battery," Abstract No. 6, Spring Meeting of the Electrochemical Society, Washington, D. C., 1976.
36. Duranti, T. R. M. S. Thesis Under progress, School of Engineering and Applied Science, University of California, Los Angeles, 1976.

DISTRIBUTION LIST

	<u>No. Copies</u>		<u>No. Copies</u>
Office of Naval Research Arlington, Virginia 22217 Attn: Code 472	2	Defense Documentation Center Building 5, Cameron Station Alexandria, Virginia 22314	12
Office of Naval Research Arlington, Virginia 22217 Attn: Code 1021P	6	U.S. Army Research Office P.O. Box 12211 Research Triangle Park, NC Attn: CRD-AA-IP	
ONR Branch Office 536 S. Clark Street Chicago, Illinois 60605 Attn: Dr. George Sandoz	1	Commander Naval Undersea R & D Center San Diego, California 92132 Attn: Technical Library Code 133	1
ONR Branch Office 715 Broadway New York, New York 10003 Attn: Scientific Dept.	1	Naval Weapons Center China Lake, California 93555 Attn: Head, Chemistry Div.	1
ONR Branch Office 1030 East Green Street Pasadena, California 91106	1	Naval Civil Engineering Laboratory Port Hueneme, California 93041 Attn: Mr. W. S. Haynes	1
ONR Branch Office 760 Market Street, Rm. 447 San Francisco, California 94102 Attn: Dr. P.A. Miller	1	Professor O. Heinz Dept. of Physics & Chemistry Naval Postgraduate School Monterey, California 93940	
ONR Branch Office 495 Summer Street Boston, Massachusetts 02210 Attn: Dr. L.H. Peebles	1	Dr. A. L. Slafkosky Scientific Advisor Commandant of the Marine Corps (Code RD-1) Washington, D.C. 20380	1
Director, Naval Research Laboratory Washington, D. C. 20390 Attn: Library, Code 2029 (ONRL) Technical Info. Div. Code 6100, 6170	6 1 1	Mr. J. F. McCartney Naval Undersea Center Sensor and Information Tech.Dept. San Diego, California 92132	1 1
The Asst. Secty of the Navy (R&D) Department of the Navy Room 4E736, Pentagon Washington, D.C. 20350	1	Dr. J. H. Ambrus The Electrochemistry Branche Materials Div. Research & Tech.Dept. Naval Surface Weapons Center White Oak Laboratory Silver Spring, Maryland 20910	1
Commander, Naval Air Systems Command Department of the Navy Washington, D.C. 20360 Attn: Code 310C (H.Rosenwasser)	1		

DISTRIBUTION LIST

	<u>No. Copies</u>		<u>No. Copies</u>
Dr. Paul Delahay New York University Dept. of Chemistry New York, New York 10003	1	Dr. R. A. Huggins Stanford University Dept. of Materials Science & Eng. Stanford, California 94305	1
Dr. R. A. Osteryoung Colorado State University Department of Chemistry Fort Collins, Colorado 80521	1	Dr. Joseph Singer, Code 302-1 NASA-Lewis 2100 Brookpark Road Cleveland, Ohio 44135	1
Dr. E. Yeager Case Western Reserve University Department of Chemistry Cleveland, Ohio 41106	1	Dr. B. Brummer EIC Incorporated Five Lee Street Cambridge, Mass. 02139	1
Dr. J.M. Proud GTE Laboratories Inc. Waltham, Massachusetts 02154	1	Library P.R. Mallory and Company, Inc. P.O. Box 706 Indianapolis, Indiana 46206	1
Dr. J. W. Kauffman Northwestern University Department of Materials Science Evanston, Illinois 60201	1	Dr. P. J. Hendra University of Chemistry Southampton SO9 5NH United Kingdom	1
Dr. R. A. Marcus University of Illinois Department of Chemistry Urbana, Illinois 61801	1	Dr. Sam Perone Purdue University Department of Chemistry West Lafayette, IN 47907	1
Dr. M. Eisenberg Electrochimica Corporation 2485 Charleston Road Mountain View, Ca. 94040	1	Dr. Royce W. Murray University of North Carolina Department of Chemistry Chapel Hill, NC 27514	1
Dr. J. J. Auborn GTE Laboratories, Inc. 40 Sylvan Road Waltham, Massachusetts 02154	1	Dr. G. Goodman Globe-Union Inc. 5757 North Green Bay Avenue Milwaukee, Wisconsin 53201	1
Dr. Adam Heller Bell Telephone Laboratories Murray Hill, New Jersey	1	Dr. J. Boechler Electrochimica Corporation Attn: Technical Library 2485 Charleston Road Mountain View, CA 94040	1
Dr. T. Katan Lockheed Missiles & Space Co., Inc. P.O. Box 504 Sunnyvale, California 94088	1		

DISTRIBUTION LIST

No. Copies

Dr. D. L. Warburton
The Electrochemistry Branch
Materials Div., Research & Technology Dept.
Naval Surface Weapons Center
White Oak Laboratory
Silver Spring, Maryland 20910 1

Dr. R. C. Chudacek
McGraw-Edison Company
Edison Battery Division
Post Office Box 28
Bloomfield, New Jersey 07003 1